MODELLING OF TUBERCULOSIS TRANSMISSION RISK FOR A RESEARCH FACILITY IN EMALAHLENI, SOUTH AFRICA

by

Ralf Ronald Küsel

Submitted in partial fulfilment of the requirements for the degree
Master of Engineering (Electronic Engineering)

in the

Department of Electrical, Electronic and Computer Engineering
Faculty of Engineering, Built Environment and Information Technology

UNIVERSITY OF PRETORIA

2019

SUMMARY

MODELLING OF TUBERCULOSIS TRANSMISSION RISK FOR A RESEARCH FACILITY IN EMALAHLENI, SOUTH AFRICA

by

Ralf Ronald Küsel

Supervisor(s):	Prof. I. K. Craig
Department:	Electrical, Electronic and Computer Engineering
University:	University of Pretoria
Degree:	Master of Engineering (Electronic Engineering)
Keywords:	Airborne infectious disease, epidemiology, mathematical modelling, *Mycobacterium tuberculosis*, risk of transmission

A detailed mathematical modelling framework for the risk of airborne infectious disease transmission in indoor spaces was developed. This modelling framework enables the mathematical analysis of experiments conducted at the Airborne Infections Research (AIR) facility of eMalahleni, South Africa. A model was built using this framework to explore possible causes of why an experiment at the AIR facility, from 31 August 2015 to 4 December 2015, did not produce expected results. In this experiment the efficacy of upper room germicidal ultraviolet (GUV) irradiation as an environmental control was tested. However, the experiment did not produce the expected outcome of having fewer infections in the test animal room than in the control room. The simulation results indicate that dynamic effects, caused by switching the GUV lights, power outages, or introduction of new patients, did not result in the unexpected outcomes. However, a sensitivity analysis highlights that significant uncertainty exists with risk of transmission predictions based on current measurement practices, due to the reliance on large viable literature ranges for parameters.

This work builds on the commonly used Wells-Riley equation for the circumstance of the research facility by including additional mechanisms and dynamics. The model framework is given modularly,

to assist in the manipulation of the model for different research questions that are wished to be explored using such a facility. The developed mathematical model is found useful in improving understanding of the risk of infection of airborne infectious diseases in indoor spaces, and in the theoretical exploration of the experiment. Especially the dynamics of the model helped to investigate whether the switching rate of the upper room GUV lights was adequately slow so that one room did indeed get more infectious particles than another.

LIST OF ABBREVIATIONS

AC	Air changes
AIDS	Acquired immune deficiency syndrome
AIR	Airborne Infections Research
BCG	Bacillus Calmette–Guérin
DNA	Deoxyribonucleic acid
GP	Guinea pig
GUV	Germicidal ultraviolet
M. tb	*Mycobacterium tuberculosis*
HIV	Human immunodeficiency virus
MDR	Multi-drug resistant
MPC	Model predictive control
TB	Tuberculosis
TST	Tuberculin skin test
UVGI	Ultraviolet germicidal irradiation
WHO	World Health Organisation

IMPORTANT DEFINITIONS

The important definitions for some of the common terms, used throughout the text, are given below to provide clarity and consistency when interpreting the text.

tuberculosis bacteria: bacteria that are capable of causing tuberculosis disease

tuberculosis disease: the state of an infection from tuberculosis bacteria where detrimental heath effects are experienced

tuberculosis infection: when tuberculosis bacteria are introduced into the host's system

latent tuberculosis infection: the state of an infection from tuberculosis bacteria where no detrimental health effects are experienced (the host's immune response is able to keep the infection in check)

active tuberculosis: the state of an infection from tuberculosis bacteria where tuberculosis disease is experienced

TABLE OF CONTENTS

CHAPTER 1 INTRODUCTION **1**

1.1 CONTEXT OF THE PROBLEM 1

1.2 PROBLEM STATEMENT 2

1.3 RESEARCH OBJECTIVE AND QUESTIONS 2

1.4 APPROACH 2

1.5 RESEARCH CONTRIBUTION 3

CHAPTER 2 LITERATURE STUDY **4**

2.1 CHAPTER OVERVIEWS 4

2.2 MICROBIOLOGICAL CLASSIFICATION 5

2.2.1 Bacteria 5

2.2.2 Actinobacteria 6

2.2.3 Corynebacterineae 6

2.2.4 *Mycobacterium* 7

2.2.5 *Mycobacterium tuberculosis* complex 7

2.2.6 *Mycobacterium tuberculosis* subspecies 8

2.3 TRANSMISSION OF *MYCOBACTERIUM TUBERCULOSIS* 8

2.4 PATHOGENESIS 9

2.5 STATES OF TUBERCULOSIS INFECTIONS 10

2.6 TYPES OF TUBERCULOSIS ACTIVE DISEASE 10

2.7 SYMPTOMS OF PULMONARY TUBERCULOSIS 11

2.8 DIAGNOSIS AND TESTING 12

2.9 TREATMENT 13

2.9.1 Treatment of active (non drug-resistant) TB 13

2.9.2 Treatment of drug-resistant TB 14

2.9.3 Treatment of latent TB . . . 14
2.9.4 Bacillus Calmette–Guérin vaccine . . . 14
2.10 EPIDEMIOLOGY AND RISK OF TRANSMISSION . . . 15
2.11 AIRBORNE INFECTIOUS DISEASE RESEARCH FACILITIES . . . 16
2.12 CONTROL ENGINEERING AND INFECTIOUS DISEASES . . . 17

CHAPTER 3 RISK OF TRANSMISSION MODELLING FRAMEWORK . . . 19
3.1 CHAPTER OVERVIEW . . . 19
3.2 RISK OF TRANSMISSION MECHANISMS . . . 19
3.2.1 New infections in the susceptible populations . . . 21
3.2.2 Infections without an incubation period . . . 22
3.2.3 Infections with an incubation period . . . 23
3.2.4 Generation of infectious particles . . . 24
3.2.5 Dispersion and distribution of infectious particles . . . 25
3.2.6 Removal of infectious airborne particles through air filtration . . . 26
3.2.7 Removal of infectious airborne particles using GUV lights . . . 27
3.2.8 Modelling assumptions . . . 27

CHAPTER 4 AIRBORNE INFECTIONS RESEARCH FACILITY MODEL AND SIMULATION . . . 29
4.1 CHAPTER OVERVIEW . . . 29
4.2 EMALAHLENI AIR FACILITY MODEL . . . 29
4.3 GERMICIDAL ULTRAVIOLET IRRADIATION STUDY . . . 33
4.4 STUDY PARAMETER ESTIMATION . . . 36

CHAPTER 5 RESULTS AND DISCUSSION . . . 42
5.1 CHAPTER OVERVIEW . . . 42
5.2 GUINEA PIG POPULATION SIMULATION RESULTS . . . 42
5.3 INFECTIOUS PARTICLE SIMULATION RESULTS . . . 43
5.4 SENSITIVITY OF THE SIMULATION PARAMETERS . . . 46
5.5 SUPER-SPREADERS AND THE STUDY . . . 53
5.6 SIMULATION FIT AND EXPERIMENT OUTCOME . . . 57

CHAPTER 6 CONCLUSION . . . 59
6.1 CONCLUDING REMARKS . . . 59

6.2 RESEARCH QUESTION ANSWERS 61
6.3 SUGGESTIONS FOR FURTHER WORK 61

REFERENCES **63**

ADDENDUM A AIR MODEL DIFFERENTIAL EQUATION SOLUTION **77**
A.1 INFECTIOUS PARTICLES IN THE WARD 77
A.2 INFECTIOUS PARTICLES IN THE ANIMAL ROOMS 78

CHAPTER 1 INTRODUCTION

1.1 CONTEXT OF THE PROBLEM

Tuberculosis (TB) remains a severe health threat in the world, despite advances in treatment and diagnosis in the past decade [1]. In South Africa especially, there is a call to improve the public health response [2]. Of significant importance in the reduction of incidence is the interruption of transmission [3, 4]. The disease is caused by the *Mycobacterium tuberculosis (M. tb)* pathogen, and the main method of transmission is via aerosoled droplets that are expelled through the respiratory tract of a host [5].

The global tuberculosis epidemic is a major cause for concern. Nine million people developed active tuberculosis and 1.5 million deaths were attributed to tuberculosis in 2013 [6]. Tuberculosis is one of the most common causes of death due to a single infectious disease [7] and places an enormous burden on the global community, especially in South-East Asia, Sub-Saharan Africa and Eastern Europe [8]. The lack of availability and affordability of health care is a barrier to the effective treatment of infectious diseases, especially in low and middle income countries [9]. In 2014, the funding gap was almost US$ 2 billion, which was 21.25 % short of the required amount [6].

Quantifying the risk of transmission of airborne infectious diseases is useful in the evaluation of the effectiveness of an infection control strategy. As an infection control strategy, rapid active case finding of infected individuals and community intervention is the more effective method [10–12]. However, active case-finding is much more expensive than the alternative passive case-finding [13]. Therefore, environmental control, such as ventilation and ultraviolet germicidal irradiation (UVGI), remains an important consideration for the reduction of the risk of transmission of an airborne infectious disease [14, 15]. Environmental factors are especially important in the time between infection and diagnosis of the infection. Although the time from the initiation of treatment to the time the treatment renders the

individual non-infectious can be rapid [16], for the reduction in risk of infection, environmental factors are also important, especially in nosocomial settings.

A mathematical model can serve as an effective tool to quantify the risk of transmission of airborne infectious diseases [17]. Mathematical models not only help in understanding, but have the advantage that an exploration of a theoretical concept through mathematical simulation is typically quicker and cheaper than conducting an experiment [18, 19]. Simulation can thus be used to increase the chance of a successful experiment by identifying potential problem areas before the start of the experiment. Mathematical models are an important part of the design of intelligent systems, where quantitative models help to gain a deeper understanding of the process involved and allow for systematic design of appropriate responses to the problem [20].

1.2 PROBLEM STATEMENT

The Airborne Infection Research (AIR) facility in eMalahleni conducts experiments on different aspects of the infectious disease: Tuberculosis (TB). A mathematical model can be used in this facility to assist in the prediction and analysis of experiments.

1.3 RESEARCH OBJECTIVE AND QUESTIONS

The objective of the research will be to use a control engineering approach to model the risk of transmission within the AIR facility. The goal of the model is to produce a representation of the risk of transmission within the AIR facility that can be used to analyse an experiment conducted at the facility. The goal of the analysis will be to investigate why the experiment conducted from 31 August 2015 to 4 December 2015 did not produce the results that were expected. The expected result was that fewer infections would have been found in animal room 1, which was the control room, as opposed to animal room 2, which had the test environmental control intervention.

1.4 APPROACH

The systematic approach that will be taken to meet the research goals, will begin with the modelling process. To create the model, different mechanisms and their respective models will be investigated. This will create the building blocks from which the model for the facility can be constructed. This

approach will be used to allow for these mechanisms to be used in the construction of a model for a different scenario.

Data from an experiment, that was conducted at the AIR facility, will be used to create a simulation of the experiment. Parameters, and parameter ranges, will be obtained from literature. A parameter estimation will be performed to fit parameters, within their literature ranges, with the objective to minimise the difference between the experiment and simulation results. This will then serve as the baseline of the parameters that will be used for the simulation.

In addition to using literature to build a model framework and a model for the facility, the time to steady state will be investigated. Additionally, a sensitivity analysis will be conducted, as well as considering the scenario of having a super-spreader.

1.5 RESEARCH CONTRIBUTION

This research will contribute to the modelling of the risk of transmission, by providing a clear summary of different mechanisms. A method for the use of the mechanisms, as basic building blocks, will be provided to allow the creation of risk of transmission models for different situations. A model for the AIR facility will be created and provided. A parameter estimation is performed to identify the quanta generation per infector for the experiment conducted at the AIR facility from 31 August 2015 to 4 December 2015. The research also helps investigate why that experiment did not produce the results that were expected.

This research contributes to scientific literature through a peer reviewed article and a conference article:

- R. R. Küsel, I. K. Craig, and A. C. Stoltz "Modelling the airborne infection risk of tuberculosis for a research facility in eMalahleni, South Africa," *Risk Analysis*, Vol. 39, No. 3, 2019, pp. 630–646.
- D. Strydom, R.R. Küsel, and I.K. Craig "When is it appropriate to model transmission of tuberculosis using a dose response model?" *IFAC-PapersOnLine*, Vol. 50, No. 2, pp. 31-36, 2017.

CHAPTER 2 LITERATURE STUDY

2.1 CHAPTER OVERVIEWS

This chapter will provide background for insight into the problem of understanding the pathogen that is investigated in this text. To develop this understanding, the properties of this disease will be the focus of this chapter. However, the background on the context of how control engineers can contribute to the body of science in understanding and combating this disease will also be provided. Additionally, the epidemiology of the disease will be discussed, which will lead into the rest of the text.

Tuberculosis (TB) is an infectious bacterial disease that can cause serious illness and is potentially fatal when left untreated [5]. *Mycobacterium tuberculosis* is the predominant causative agent of tuberculosis disease in humans [21]. In general, TB is an airborne infectious disease that is spread when a person that has active TB expels the pathogen in aerosol droplets from the respiratory tract. When the expelled, aerosol droplets containing the pathogen are inhaled by an uninfected person the bacteria can cause infection.

To describe the disease in more detail, several different concepts of tuberculosis must be discussed. These are:

1. microbiological classification,
2. transmission,
3. pathogenesis,
4. types of tuberculosis disease,
5. symptoms,
6. diagnosis and testing, and

7. treatment.

The microbiological classification is the first concept discussed, because this provides background to the properties of the bacteria.

2.2 MICROBIOLOGICAL CLASSIFICATION

Characteristics of the causative agent, *Mycobacterium tuberculosis*, can be explained through the taxonomy, which categorises organisms into named groups (taxon) based on shared characteristics. Because the taxa have a hierarchical rank, the characteristics of each taxon, the organism is categorised under, are applicable to that organism. The general hierarchical rankings are: kingdom, phylum, class, order, family, genus and species; however, rankings of phylum is not applicable to the kingdom Bacteria [22]. The taxonomy of *Mycobacterium tuberculosis* is given in Table 2.1 down to the rank of species.

Table 2.1. The hierarchical rankings for the taxonomy of *Mycobacterium tuberculosis*.

Kingdom	Bacteria
Class	Actinobacteria
Order	Corynebacteriales
Family	Mycobacteriaceae
Genus	*Mycobacterium*
Species	*Mycobacterium tuberculosis*

The different characteristics of the taxa from Table 2.1 are discussed in more detail below.

2.2.1 Bacteria

Bacteria are unicellular organisms that have an organisation of the chromosome as a nucleoid in the cytoplasm without an endomembrane [23]. This means that, although bacteria have a cell wall, there is no membrane separating the genetic material in the cell. Recombination of bacteria is characterised by a parasexual processes [23].

Most bacteria reproduce through the mechanism of binary fission [24]. This is an asexual reproduction process where the cell grows until it divides in half. The process begins with a replication of the

chromosome. As the deoxyribonucleic acid (DNA) is copied through the replication process, the cell elongates. Once the entire chromosome has been replicated and separated, the cell wall pinches inward. This then results in the division into two new cells, which means that the growth rate of bacteria, under favourable conditions, is exponential.

2.2.2 Actinobacteria

Actinobacteria are characterised as being Gram-positive bacteria with a high proportion of guanine and cytosine content in their DNA [25]. Gram-positive bacteria have multiple, thick peptidoglycan layers in the cell wall, as opposed to Gram-negative bacteria that have only a narrow peptidoglycan layer in the cell wall. Peptidoglycan is a polymer consisting of amino acids (peptido-) and sugars (-glycan) that has a mesh-like organisation.

The Gram stain test uses crystal violet to suffuse a sample with colour. Gram-positive bacteria withhold the stain and give the sample a purple appearance under a microscope. The Gram stain test is used to quickly classify bacteria into two broad categories [26].

The type of cell wall is an important characteristic affecting the toxicity and anti-biotic responses of the bacterium. For example, the bactericidal antibiotic penicillin impedes the cell membrane growth, which leaves the cell vulnerable to destruction through osmosis because the the bacterial cell is generally more salty than its environment.

2.2.3 Corynebacterineae

The Corynebacterineae are characterised as being acid-fast bacteria. In *Mycobacterium tuberculosis* this is due to the high mycolic acid content in the cell wall [27]. Isoniazid is a bactericidal first-line tuberculosis antibiotic, which inhibits the mycolic acid synthesis of the cell wall of the bacterium cell, causing it to die.

Acid-fast bacteria are resistant to the decolourisation by an acid solution. This causes the bacteria to retain the original stain colour after the sample has been decolourised by an acid solution, whereas the rest of the sample will not retain the stain colour.

2.2.4 *Mycobacterium*

Mycobacteria are the only genus in the family Mycobacteriaceae, and are characterised as being aerobic (requiring oxygen), non-motile (incapable of motion) and rod-shaped [28]. *Mycobacterium* are the causative agents of two major diseases in humans: tuberculosis and leprosy.

2.2.5 *Mycobacterium tuberculosis* complex

Although *Mycobacterium tuberculosis* is the predominant causative agent of tuberculosis in humans, it is not the only *Mycobacterium* species that can cause tuberculosis disease. The *Mycobacterium tuberculosis* complex is a group of genetically related *Mycobacterium* species that can all cause tuberculosis disease. Most of the *Mycobacterium tuberculosis* complex species have different biological hosts, but can still cause tuberculosis disease in humans through zoonotic transmission. In Table 2.2 the different species in the complex are given, together with their typical hosts.

The transmission of zoonotic tuberculosis occurs through close contact with infected animals or consumption of contaminated animal products, such as unpasteurized milk [29]. Of the zoonotic forms of tuberculosis, most cases are as a result of transmission from cattle, and the primary causative agent is *Mycobacterium bovis* [21]. The treatment of *Mycobacterium bovis* is made more challenging, because *Mycobacterium bovis* is innately resistant to pyrazinamide, which is one of the first line drugs used to treat tuberculosis. However, tuberculosis disease caused by transmission of *Mycobacterium tuberculosis* is significantly more prevalent in humans than zoonotic transmission, with about 98% of TB cases being caused by *Mycobacterium tuberculosis* [21]. Therefore, this text will further only focus on tuberculosis caused by the *Mycobacterium tuberculosis* pathogen.

Table 2.2. The *Mycobacterium tuberculosis* complex species, and the host in which they are predominantly found.

Species	Host
Mycobacterium africanum	Humans
Mycobacterium bovis	Cattle
Mycobacterium canetti	Unknown [30]
Mycobacterium caprae	Cattle or goats [31]
Mycobacterium microti	Vole, cats or lamas
Mycobacterium mungi	Mongoose [32]
Mycobacterium orygis	Bovidae [33]
Mycobacterium pinnipedii	Seals [34]
Mycobacterium suricattae	Meerkat [35]
Mycobacterium tuberculosis	Humans

2.2.6 *Mycobacterium tuberculosis* subspecies

Although the main properties of the organism is explained through the species, the different genetic variants are classified into subspecies, with strains being a grouping of these subspecies. The subspecies of *Mycobacterium tuberculosis* (*M. tb*) are not detailed in Table 2.1 because the number of variations is too numerous for this text to consider all of them. However, it is important to note that the different strains of *Mycobacterium tuberculosis* have a variation in pathogenity [36], meaning that the ability to cause disease varies between these different subspecies. The drug-resistance of some tuberculosis infections is also attributed to the genetic differences between *Mycobacterium tuberculosis* strains [37–39].

2.3 TRANSMISSION OF *MYCOBACTERIUM TUBERCULOSIS*

TB is an airborne disease and is spread through aerosol infectious *Mycobacterium tuberculosis* pathogens that are expelled from the respiratory tract of an individual with active TB disease. A single viable TB bacillus, once inhaled, can be sufficient to produce infection [40].

Respiratory actions such as breathing, coughing, sneezing, speaking, singing, and spitting all expel particles from the respiratory tract, with the quantity and size distribution of these particles varying

between these different actions and between individuals [41,42]. The smaller expelled particles tend to remain airborne for much longer periods than the larger expelled particles. The average size of droplet nuclei from a cough is between 0.6 - 5.4 μm [43], where a size of less than 10 μm is considered a 'small' particle [44]. From a cough-generated aerosol experiment, it was found that coughing can generate between 18 to 3798 infectious *M. tb*, 'small' droplet particles per hour from individuals with active disease [41].

Tuberculosis is typically infectious as an active disease, from the onset of coughing until about two weeks after treatment has started [45]. However, the health of a patient influences their contagiousness, as there is some correlation between the bacillus count in a sputum smear analysis and the infectiousness of the patient. A delay in diagnosis and treatment therefore affects transmission [46,47].

2.4 PATHOGENESIS

Pathogenesis describes the manner in which the disease develops. With *Mycobacterium tuberculosis*, the infection begins with the deposition of the bacteria in the alveoli after inhalation of an aerosol droplet containing the bacteria [48,49]. Here the pathogen encounters the host's innate immune response, and is ingested by the alveolar macrophages.

Macrophages are white blood cells which engulf foreign material that does not present proteins of the host on the surface of the material. Once the foreign material is ingested by the macrophage, it gets disassembled by being fused with the lysosome, which is an organelle that contains hydrolytic enzymes. After the foreign material has been dissembled, it is presented by the macrophage as an antigen to engage the adaptive immune response. The antigens stimulate T helper cells, which in turn produce cytokines that stimulate cytotoxic T cells, antibody producing B cells and activate phagocytes, like macrophages, to be more bactericidal [50–52]. This complex process of the innate and adaptive immune system is necessary for the body to be able to appropriately respond to, and remove, pathogens while not destroying the body's own cells.

With *Mycobacterium tuberculosis*, however, the macrophage is often not able to dissemble the bacteria, but instead the bacteria is able to replicate in the cell. In this case, the bacteria eventually kills the infected macrophage, releasing the now multiplied bacteria. However, cytotoxic T cells are able to kill the extracellular bacteria, and are able to disintegrate infected macrophages [53]. Additionally,

through the cytokines interferon gamma and tumour necrosis factor, macrophages are activated to kill *Mycobacterium tuberculosis* [49]. Immune cells recruit to the site of infection, and attempt to wall in the bacteria. This is known as a granuloma. The centre of the granuloma begins to form caseous necrosis, which is a collection of dead cells and tissue that have the appearance of soft, white cheese. If the bacteria is cleared, such as through treatment, then necrotic tissue heals with scarring and calcification.

2.5 STATES OF TUBERCULOSIS INFECTIONS

Upon primary infection with *Mycobacterium tuberculosis*, the immune system is usually able to suppress the infection, and after mild flu-like symptoms, the recovery process usually begins [54]. However, in about 5 % of TB infections, the host immune response is not able to suppress the infection and the primary infection progresses into a state of active disease. This active disease can be classified as a number of different types, based on the site formation of granulomas in the body.

However, in the other 95 % of primary infections, the bacilli are not completely eradicated by the immune system, and the bacilli are in a stalemate with the immune system, the infection remains dormant [55]. While the tuberculosis infection is dormant, this state of infection is known as a latent TB. An individual may be latently infected with TB for the duration of their lives without ever experiencing further symptoms.

However, from its latent state, the tuberculosis infection may become reactivated, and this happens to approximately another 5 % of the individuals that were infected. The risk of reactivation greatly increases in immunocompromised individuals [5, 54]. For this reason, the tuberculosis epidemic increased with the emergence of the human immunodeficiency virus (HIV) epidemic [56].

2.6 TYPES OF TUBERCULOSIS ACTIVE DISEASE

Several different types of TB disease exist; however, the different types can be categorised into two broad groups:

1. pulmonary TB, and
2. extrapulmonary TB.

Pulmonary TB is the infection of the lungs, whereas extrapulmonary TB is when the infection occurs outside the lungs. Extrapulmonary TB can affect almost any organ system in the body [57], and often results from hematogenous dissemination of the pathogen, meaning that the bacteria is spread via the bloodstream. In Table 2.3 the most common forms of extrapulmonary tuberculosis are listed.

Pulmonary TB is the most common form (and more common group) of TB disease, because TB is usually airborne transmitted, making the lungs the initial site of infection. However, both extrapulmonary and pulmonary TB infections may also occur simultaneously. The simultaneous manifestation of pulmonary and extrapulmonary TB is the most common manifestation of TB disease in HIV positive people [58]. This text, however, will focus on pulmonary tuberculosis, because it is the more important in the consideration of the transmission of the pathogen.

Table 2.3. The most common forms of extrapulmonary tuberculosis [57].

Name	**Site of infection**
Abdominal tuberculosis	gastrointestinal tract, liver, spleen or pancreas
Bone and joints tuberculosis	bones or joints
Genitourinary tuberculosis	kidneys, bladder or genitals
Lymph node tuberculosis	lymph nodes
Miliary tuberculosis	an infection that has spread to two or more sites
Tuberculous meningitis	central nervous system
Tuberculous pleurisy	layers of tissue around the lungs

2.7 SYMPTOMS OF PULMONARY TUBERCULOSIS

The typical symptoms that characterise the onset of pulmonary TB are fatigue, weight loss and a persistent cough. As the individual's health condition worsens, these symptoms can extend to chest pains, fever and night sweats. There may also be blood in the coughed up sputum, where sputum is a mixture of saliva and mucus. The sputum and blood from the infection are caused by the caseous necrosis in the granulomas. The initial symptoms are similar to other respiratory infections, making tuberculosis difficult to diagnose from the symptoms [46].

2.8 DIAGNOSIS AND TESTING

A patient who is exhibiting some or all of the symptoms of tuberculosis disease, should obtain assistance from a medical professional. Many of the symptoms are similar to other respiratory diseases, such as the common cold or influenza; however, there are some clinical differences from which a medical professional could suspect a tuberculosis infection. If a tuberculosis infection is suspected, then there are various tests that can be performed in an attempt to obtain a positive identification. The different types of tests can be grouped as:

- a chest x-ray,
- a tuberculin skin test,
- sputum smear microscopy,
- a culture test, and
- interferon gamma release assay.

A chest x-ray can show the signs of pulmonary tuberculosis disease because large granulomas can appear as abnormal shadows on the lungs. However, this test is not specific because these abnormal shadows are not conclusive proof of a tuberculosis infection, and should be used in conjunction with other testing methods. Although this method is not specific, it is often used as a screening method because it is relatively quick to administer and yield results.

The tuberculin skin test (TST) can identify a tuberculosis infection, but does not indicate whether the infection is latent or active. For the test, an intradermal injection of tuberculin is administered, with the intent to monitor the skin's response at the site of the injection. Tuberculin is a purified protein derivative that is made out of *M. tb*. If the host has a tuberculosis infection, the skin will react by forming a raised and hardened area, known as an induration, at the site of the injection. After a waiting period of two to three days, the diameter of the induration is measured, and a classification is made based on medical risk factors. However, the test can give a false positive if a person previously received the Bacillus Calmette–Guérin (BCG) vaccine or due to nontuberculosis mycobacteria. Although this method does not give a conclusive positive, it is often used as a screening method because it is relatively quick to administer and yield results.

Sputum smear microscopy can quickly identify tuberculosis disease, but is only $50-60\%$ sensitive [59]. For the test, samples of sputum are collected, smeared onto a thin glass slide, stained and analysed using a microscope. Sputum is a mixture of saliva and mucus that is coughed up from the respiratory tract. The stain that is used highlights acid-fast bacteria, allowing the *M. tb* bacteria to be seen more easily under a microscope.

A culture test involves first growing the bacteria before analysing them under a microscope. Sputum samples, with suspected tuberculosis bacteria, are placed on culture media and allowed to incubate. To test the drug susceptibility of this particular bacterial sample, the bacteria is grown in the presence of diluted solutions of the different drugs. If the bacteria is able to successfully grow in the presence of the drug, it is resistant to this drug. Although culturing is a more accurate method and can give drug susceptibility results, it takes several weeks for the test to be completed.

The interferon gamma release assay can be used to diagnose TB infection by detecting interferon gamma cytokines, that are produced by the immune system in response to a TB infection. This method is more accurate than the TST, and does not cross react with the BCG vaccine; however, it also cannot distinguish between active or latent tuberculosis.

2.9 TREATMENT

Tuberculosis is a curable disease, and is treated through the use of antibiotic drugs. However, the selection of the antibiotic drug regimen and course length, depend on the form of the disease and the strain of the bacteria. The treatment for latent tuberculosis is different to the treatment for active tuberculosis disease. Additionally, if the bacterial strain is resistant to some antibiotic drugs, then the regimen must be carefully selected so as to still be effective. The treatment of tuberculosis therefore starts with positive diagnosis of the disease, and ideally with some drug-susceptibility testing of the bacterial strain.

2.9.1 Treatment of active (non drug-resistant) TB

In the case of drug-susceptible tuberculosis, the first line antibiotic drug regimen is prescribed. The first line drugs are the combination of anti-tuberculosis drugs that are most effective, while having the least severe side-effects. The World Health Organisation recommends treatment as a six month

course, where the first two months are with the drugs: Isoniazid, Rifampicin, Pyrazinamide and Ethambutol. The last four months of the treatment are with just Isoniazid and Rifampicin [60]. It is important that patients comply with the prescribed treatment and complete the course fully, otherwise there is a significant risk that the bacteria will mutate into a strain that is resistant to the administered antibiotics [39].

2.9.2 Treatment of drug-resistant TB

There are two different classifications for drug-resistant tuberculosis: multi drug-resistant and extensively drug-resistant. Tuberculosis is classified as being multi drug-resistant when the bacteria is resistant to either of the first line drugs, Isoniazid or Rifampicin. In multi drug-resistant cases, the second line drugs must be administered. The drug regimen for multi drug-resistant tuberculosis depends on the drug resistance, but should combine at least four different antibiotics, and should be continued for at least four months after the patient tests negative [60].

Extensively drug-resistant tuberculosis is the classification of an infection with bacteria that is resistant not only to the first line drugs Isoniazid and Rifampicin, but also to at least two of the second line drugs. Extensively drug-resistant tuberculosis has a very low survival rate and the side-effects of the drugs are also severe.

2.9.3 Treatment of latent TB

Latent tuberculosis can be cured, and is typically done with a Isoniazid for nine months, or Isoniazid and Rifapentine for three months. However, if the patient has known contacts with drug-resistant tuberculosis, the treatment regimen is modified. Latent tuberculosis should be treated if the patient has a higher risk of contracting active tuberculosis, such as HIV positive patients.

2.9.4 Bacillus Calmette–Guérin vaccine

The Bacillus Calmette–Guérin (BCG) vaccine is the only vaccine against tuberculosis. Although the vaccine is not very effective in adults, it does provide protection to children against disseminated forms of tuberculosis disease. The vaccine is produced out of *Mycobacterium bovis* that is attenuated so that it loses its ability to cause disease in humans; however, it is still able to confer some immunity against

Mycobacterium tuberculosis.

2.10 EPIDEMIOLOGY AND RISK OF TRANSMISSION

Epidemiology is the study of the occurrence and distribution of health-related events, states, and processes in populations, and the application of this knowledge to the prevention and control of health-related problems [61]. In 2003 it was estimated that approximately a third of the population of the world was infected with *Mycobacterium tuberculosis* [56]. Although only 5% to 10% of those that are infected with *Mycobacterium tuberculosis* actually develop active tuberculosis disease in their lifetime [5, 52, 54], this estimate still indicates that tuberculosis is a major health problem.

More recent statistics of the global tuberculosis burden indicate that in 2017 TB was one of the top ten leading causes of death, and the number one cause of death due to a single infectious agent [62]. The estimated incidence of tuberculosis in 2017 was that 10 million people got sick with tuberculosis disease [62]. Although the disease is curable, the estimated mortality in 2017 was that 1.57 million people still died due to tuberculosis [62]. To establish the incidence of tuberculosis, a re-estimate of the global latently infected population was done in 2014, and indicated that approximately 23% of people are latently infected [63].

Epidemiology of tuberculosis involves a number of different aspects that contribute towards combating the incidence and mortality of tuberculosis [64]. The main aspects of tuberculosis epidemiology include

- identifying risk factors for the transmission and activation of tuberculosis infections,
- identifying the individuals or networks at greatest risk of disease,
- identifying, evaluating and supporting public health interventions, and
- obtaining and communicating the public health information.

However, the aspect that is of greatest interest for this text, is the study of the risk factors influencing the transmission of the disease. Because *M. tb* is primarily transmitted through the airborne route, there is great benefit in understanding and implementing measures to control this route of infection.

In the study of airborne infectious diseases, animals are often used as a method of detecting the risk to humans [65]. Human to guinea pig transmission is a common method that is used to study air disinfection techniques [66–70]. This usually requires the sentinel animal to be placed in a different room to the source of the pathogen, with mechanical ventilation used as a proxy for the risk of infection in the ward.

This method of studying the risk of transmission of airborne diseases goes back to the experiments by William F. Wells between 1930 and 1955 to identify whether pathogens can indeed be truly airborne [71]. Together with his protégé Richard L. Riley, they formulated an equation to quantify the risk of transmission for indoor spaces. The Wells-Riley equation [72] remains the most commonly used model to quantify the risk of transmission for indoor spaces [17]. However, the Wells-Riley equation is limited to situations in which the infected individuals are in the same zone as the susceptible individuals [73]. These assumptions make the Wells-Riley equation not actually hold for the modelling of airborne infectious disease research facilities where the sentinel animals are not in the same airspace.

2.11 AIRBORNE INFECTIOUS DISEASE RESEARCH FACILITIES

The first airborne infectious disease research facility for the study of tuberculosis was created by William F. Wells and Richard L. Riley in 1954 at a hospital in Baltimore, United States of America [40, 66, 74]. The purpose of this facility was to prove tuberculosis is infectious via the respiratory route. This was done by observing whether guinea pigs, that were breathing air vented from the six person tuberculosis ward in the hospital, would become infected.

The facility had two animal chambers in the penthouse of the hospital, which housed the guinea pigs that were used as sentinel animals. The ventilation system of the tuberculosis ward was designed to channel the suspected infectious ward air over the guinea pig chambers. However, the air to one of the two chambers was irradiated with ultraviolet light for disinfection, and the animals in this chamber served as the control group. For the duration of the study, regular sputum culturing was performed on the human patients, and patients with sputum negative results were moved out of the ward and replaced with patients with sputum positive results. The guinea pigs were tested on a monthly basis using the tuberculin skin test method. The results of the experiments conducted at this facility proved the hypothesis that tuberculosis is transmitted via the airborne route.

Following the proof that some infectious diseases are transmitted via the airborne route, research on tuberculosis as an airborne infectious disease has been further conducted at multiple different facilities on a laboratory scale (such as [75–77]). However, in this text, facilities studying the transmission of wild strains of tuberculosis will be focused on. As such, the next major research facility for the study of tuberculosis was built at the Hospital Nacional Dos de Mayo in Lima, Peru [69]. The facility was similar in design to that of Wells and Riley, and was used to conduct research on the airborne transmission of tuberculosis by patients co-infected by HIV and environmental controls.

Shortly after the creation of the facility in Peru, another was built next to the tuberculosis hospital in Emalahleni, South Africa [70]. This facility too was based on the design of Wells and Riley, with two animal chambers that receive ventilated air from a tuberculosis ward with infectious human patients. The main purpose of this facility was the study of multi-drug resistant tuberculosis airborne transmission and environmental controls. This facility is where the research covered in this text was conducted, and will be further detailed in subsequent chapters.

2.12 CONTROL ENGINEERING AND INFECTIOUS DISEASES

In the case of infectious diseases, not only is the effect on an individual important, but also the effect on the population. Epidemiology and networks of directly transmitted infectious diseases are fundamentally linked, because an individual has a finite number of contacts to whom the infection can be passed [78]. Thus, the control of the disease for an individual, could have implications for the population as a whole. By considering the individuals' response to infection in the context of a population, it has been shown in an HIV contact network that by 'controlling' certain individuals, the spread throughout the population can be controlled [79]. Because the effect on the population is important, for airborne infectious diseases it is useful to quantify the risk of transmission of the pathogen.

Quantifying the risk of transmission can also be useful in the evaluation of the effectiveness of an infection control strategy. As an infection control strategy, rapid active case finding of infected individuals and community intervention is the more effective method [10–12]. However, active case finding is much more expensive than the alternative passive case finding [13]. Therefore, environmental control, such as ventilation and germicidal ultraviolet (GUV) lights, remains an important consideration for the reduction of the risk of transmission of an airborne infectious disease [14, 15]. Environmental

factors are especially important in the time between infection and diagnosis of the infection. Although the time from the initiation of treatment to the time the treatment renders the individual non-infectious can be rapid [16], for the reduction in risk of infection, environmental factors are also important, especially in nosocomial settings.

A mathematical model can serve as an effective tool to quantify the risk of transmission of airborne infectious diseases [17]. Mathematical models not only help in understanding, but have the advantage that an exploration of a theoretical concept through mathematical simulation is typically quicker and cheaper than conducting an experiment [18, 19]. Simulation can thus be used to increase the chance of a successful experiment by identifying potential problem areas before the start of the experiment. Mathematical models are an important part of the design of intelligent systems, where quantitative models help to gain a deeper understanding of the process involved and allow for systematic design of appropriate responses to the problem [20].

With a mathematical model, control engineering can help with the study of diseases by considering them as a dynamic process that can be considered by both its transient and steady-state behaviour [80]. In this way, control systems' knowledge basis and methods can be applied to the modelled problem to give a different perspective on the disease. Some examples of this are:

- Optimal control of epidemics [81]
- Feedback systems for drug delivery [82]
- HIV/AIDS control and optimal initiation of therapy [18, 19]
- Selective pinning control in an HIV contact network [79]

However, the first step to being able to apply this control engineering knowledge, is to model the process. The subsequent chapters will establish the model, and use it to analyse a medical experiment.

CHAPTER 3 RISK OF TRANSMISSION MODELLING FRAMEWORK

3.1 CHAPTER OVERVIEW

In this chapter, a framework for developing and manipulating a risk of transmission model for an indoor space, and specifically for an airborne research facility, will be outlined. This will then be used in the subsequent chapter to create a model to analyse a specific experiment in an airborne research facility.

3.2 RISK OF TRANSMISSION MECHANISMS

The approach to model development that is followed by this text, is one of defining multiple different effects of the risk of transmission within indoor spaces as individual mathematical descriptions. These mathematical descriptions can then be combined. Where the mechanisms are linear, the law of superposition is applicable; where the mechanisms are nonlinear, an alternative approach is given. This allows freedom to construct relevant models for different situations and research questions.

The model will be given in a deterministic, mechanistic, nonlinear state-space and continuous time format. Mechanistic physical laws are used to define the model, instead of using empirical modelling to fit data. The deterministic model represents an average expected risk of transmission, which is assumed to be the same as the average of an equivalent stochastic model. The deterministic model is chosen as opposed to a stochastic probabilistic model [83] or a Markov chain model [84]. As a result of using the expected risk of transmission, the modelling process will be simplified by removing the need to specify the uncertainty through the definition of random variable distributions in the model.

The probability that the pathogen deposits on the alveolar of an individual follows a Poisson distribution [40, 85]. This probability distribution is described through an exponential function, similar to the result of solving a linear differential equation. Since other influencing factors on the risk of transmission can be expressed in terms of rates of change, this allows for the use of differential equations to describe the model.

A convenient way in which to represent a model is the state-space format that relates the inputs and state variables through simultaneous, first-order differential equations. An advantage of the state-space format is its relevance in control systems theory, which can assist in the study of infectious diseases [19, 79, 86]. Methods for parameter extraction are well developed in control systems theory, and provide tools for determining unknown parameters in a model from measurements [87–89]. The Gammaitoni-Nucci model also follows a state-space format [90] and, in contrast to the Wells-Riley equation, allows for the consideration of non-steady state conditions of airborne infectious particles [91].

Within the state-space format, the state variables are the smallest subset of system variables that fully describe the system [92]. The determination of these system values is dependent on given initial values of the state variables and the forcing functions. Four different categories of state variables are defined for the model framework used in this paper; however, in the construction of a model, the number of state variables within each category may vary. The first category is the groups of susceptible individuals that represent the populations with the potential of being infected. The second and third categories of state variables are the groups of infected individuals and the groups of exposed individuals. The distinction between the infected and the exposed population classifications depends on the definition of infection used in the model, and whether an incubation period is included in the model [93]. The final category of state variables considered, is the number of infectious aerosol particles within a space.

Parameters in the model will be given as non-time varying to avoid confusion between parameters and state variables.

3.2.1 New infections in the susceptible populations

New infections in the susceptible population S_i, are described as an average probabilistic reduction of the susceptible population based on the expected exposure to the pathogen. Susceptible populations that are geographically separated can be defined as populations in different zones and denoted with their subscript i. A zone is an air space, which can be a room or parts of a room [73, 94].

The rate of new infections is proportional to the pulmonary ventilation rate p_i $(m^3 \cdot s^{-1})$ of the susceptible population and the concentration of infectious particles that the susceptible population is potentially exposed to [90]. The concentration of infectious particles is given as the fraction of the number of infectious particles $C_i(t)$ (quanta) over the volume V_i (m^3). An infectivity term θ_i $(quanta^{-1})$ allows for the consideration of a fraction of the re-breathed air that is inhaled, but does not cause infection, where, for example, not all of the inhaled pathogens land on alveoli [95]. The infectivity term also addresses the dimensionality problem of the Wells-Riley equation, even if it is taken as unity [17].

New infections in the susceptible populations are described mathematically, in this model framework, by:

$$\frac{dS_i(t)}{dt} = -p_i \theta_i \frac{C_i(t)}{V_i} S_i(t) \quad . \tag{3.1}$$

The use of respirators as an intervention method can be included into the model by multiplying (3.1) with an extra factor R that reduces the risk of infection based on the efficacy of the respirator [96].

The usage of the subscripts for the susceptible population or zone under consideration allows for the consideration of different susceptible populations or zones. This is because a population could be assumed to be present in more than one zone, depending on the manner in which the zones are defined. The zones could be defined as something with physical barriers, like rooms in a hospital, or as sections with different airflow, if the air is considered as not well mixed [73, 94]. When considering air that is not well mixed in a room, the susceptible population can be assumed to be exposed to infectious particle concentrations from more than one zone at the same time. The expected fraction of time spent in each of these zones f_i accounts for the susceptible population not being able to be in all the zones at the same time. The infectious particle concentrations multiplied by the expected time fraction of zone

m to n will then be summed, so that

$$\frac{dS_x(t)}{dt} = -p_x\theta_x S_x(t)\sum_{i=m}^{n} f_i\frac{C_i(t)}{V_i} \quad , \tag{3.2}$$

where the susceptible population x comes into contact with the infectious particles concentrations of zones m to n.

The pulmonary ventilation rate can also be taken as unique for each individual, then the mathematical expression can be given as

$$\frac{dS_x(t)}{dt} = -\sum_{j=1}^{N_x}\left(p_j u_{Sj}(t)\sum_{i=m}^{n}\frac{C_i(t)}{V_i}\right) \quad , \tag{3.3}$$

where $u_{Sj}(t)$ is an indicator function, and takes the value 1 when individual j is still part of the susceptible pool, but changes to 0 when that individual becomes infected. The total number of (starting) susceptibles in population x is given by N_x.

Although the option of considering air that is not well mixed was presented here, for the remainder of this text it will be assumed that the air is well mixed and that $x = i$. This simplifies the framework presentation and will be the situation that will be considered in subsequent chapters.

3.2.2 Infections without an incubation period

New infections, when no incubation period is considered, are treated as the increase of the infected population due to the average probabilistic reduction of the susceptible population based on the expected exposure to the pathogen. The rate at which the infected population grows due to exposure to the pathogen is given by

$$\frac{dI_i(t)}{dt} = p_i\theta_i\frac{C_i(t)}{V_i}S_i(t) \quad . \tag{3.4}$$

Equation (3.4) is the complement of (3.1). This ensures that the total population size remains constant when no external factors, such as birth or deaths within the population, are considered. It is assumed viable to leave out the consideration of these when modelling an airborne infectious diseases research facility.

3.2.3 Infections with an incubation period

The incubation period of the disease is important to consider when the measurement of the risk is performed using a sentinel animal. To include an incubation period, an extra epidemiological population is introduced as another state variable, namely the exposed individuals population category [93].

The exposed individuals are a hypothetical state, where the individual has been infected, but is asymptomatic. This can also mean that the individual responds negatively to the diagnosis and testing, however, this depends on the model and the situation considered.

If an incubation period is considered, then the individuals first become exposed before they transition to the infected state. The exposed population E_i then increases based on the expected exposure to the pathogen. The rate at which the exposed population grows due to exposure to the pathogen is given by

$$\frac{dE_i(t)}{dt} = p_i\theta_i\frac{C_i(t)}{V_i}S_i(t) \quad . \tag{3.5}$$

The transition from the exposed to the infected state is based on an incubation period delay rate α_x. The terms that then govern this mechanism in the exposed and the infected individuals, is given as

$$\frac{dE_i(t)}{dt} = -\alpha_i E_i(t) \tag{3.6}$$

in the exposed individuals population, and

$$\frac{dI_i(t)}{dt} = \alpha_i E_i(t) \tag{3.7}$$

in the infected individuals population.

Equation (3.5) is the complement of (3.1), and (3.6) is the complement of (3.7). This ensures that the total population size remains constant when no external factors, such as birth or deaths within the population, are considered.

3.2.4 Generation of infectious particles

Infectious particles are assumed to be generated in the airspace through the expulsion of small, pathogen-containing aerosol particles by infected individuals [44, 97, 98], with the infectivity of an airborne disease taken to be directly linked to these cough-generated aerosols [41, 47].

The infectious particles in a zone $C_i(t)$ are modelled in units quanta. A quantum of infection is defined as the number of infectious particles that would infect 63.2% (i.e. $1-e^{-1}$) of the population, if every member of the population was exposed to this quantity of infectious particles [40]. The quanta is a hypothetical infectious dose unit and describes the infectivity as well as the infectious source strength of an epidemiological outbreak [17].

The total average size distribution of coughed droplet nuclei is approximately 0.5-6 μm [43] and there is a proven increase of aerosol particles, in the region of microbial particle sizes, of 3-4 μm due to human room occupation [42]. Therefore, a direct link between the number of infected and the quantity of infectious particles in an indoor space seems reasonable.

The rate at which infectious particles are generated in a zone is proportional to the rate of quanta expelled by an individual ϕ_i ($quanta \cdot h^{-1}$). If the infectious individuals $I_i(t)$ in a zone are each assumed to generate quanta at the same rate on average, then the rate at which quanta in a zone is generated is given by

$$\frac{dC_i(t)}{dt} = \phi_i I_i(t) \quad . \tag{3.8}$$

where ϕ_i is the function that describes the generation of quanta by the infectious population $I_i(t)$ that expels quanta into zone i.

It is, however, possible to also define a different quanta generation function for each individual, such that the mathematical expression then becomes

$$\frac{dQ_i(t)}{dt} = \sum_{k=1}^{N_i} \phi_{ik}(t) w_{ik}(t) \quad , \tag{3.9}$$

where $w_{ik}(t)$ is an indicator function, and takes the value 0 when the potential infector k is not contributing to the quanta generation in a zone, and is 1 when that infector is. This means that the total

number of potential number of infectors, N_i and their infectiousness when they are infectious must be known a priori.

The quanta generation rate ϕ is backwards calculated from epidemiological data. The quanta generation rate ($quanta \cdot h^{-1}$) is in the range of $1.25 - 30\,840$ $quanta \cdot h^{-1}$, depending on the situation [90,91,99]; however, for an average TB patient, the range is between $1.25 - 12.7$ $quanta \cdot hour^{-1}$ [99]. Inherent in the backwards calculation of the quanta generation rate is the viability loss and the deposition loss of the pathogen, therefore these mechanisms should not be considered twice when using the quanta of infection [17, 100].

However, the quanta of infection does not have to be used as the unit of infectious particles, and ϕ could be set equal to an equivalent dose response function. An example of this is to set

$$\phi = G\beta \quad , \tag{3.10}$$

where G is the emission rate of pathogens per infected individual, and β the alveoli disposition fraction [101]. However, when doing so, the implications of moving from a hypothetical infectious dose unit (quanta) to an actual infectious dose unit need to be carefully considered. The viability of the aerosol pathogen, for instance, would then need to be taken into account.

3.2.5 Dispersion and distribution of infectious particles

The proximity of infected individuals to susceptible individuals, in relation to the ventilation air ducts, can be an important factor [15]. In situations where the air in the room is not well-mixed, this can be modelled by using different zones and the transfer rate of infectious particles between these zones [73, 84, 94].

The rate at which infectious particles are dispersed out of and diffuse into different zones or into the environment, is dependent on the air movement in a zone. The physical law of conservation of mass is used here as the modelling principle. This implies that infectious particles in a zone are assumed to stay in that zone unless they are removed through air movement or decay from that zone. The removal of infectious particles from a zone due to air movement is given by the mathematical expression

$$\frac{dC_i(t)}{dt} = -\frac{Q_i}{V_i} C_i(t) \quad , \tag{3.11}$$

where the function Q_i describes the airflow out of the zone in volume of air per unit time. The environment is assumed to be an unmodelled sink of the pathogens, so as to obey the conservation of mass theory.

The increase of infectious particles in zone i due to the removal of infectious particles from another zone, j, is then given by

$$\frac{dC_i(t)}{dt} = \frac{Q_j}{V_j} C_j(t) \quad \text{,where } j \neq i. \tag{3.12}$$

Equation (3.12) assumes that $Q_j(t)$ is not only the airflow out of zone j, but also the airflow into zone i. The model indirectly accounts for temperature changes between zones through the consideration of volumetric airflow, because the rate at which infectious particles are moved between zones is directly proportional to the volumetric airflow rates. Volumetric airflow rates are proportional to temperature conditions according to Charles's law, which forms part of the ideal gas law [102].

The equations for the dispersion and diffusion of infectious particles do not account for the dynamics involved in the dispersion of infectious particles from infected individuals into the zone through coughing, speaking and other respiratory expulsions [103–105]. If the zone is not well-mixed or the susceptible population is assumed to be in the same zone as the infected population, then these dynamics may be an important consideration.

3.2.6 Removal of infectious airborne particles through air filtration

The removal of infectious particles can be achieved through air filtration, if air in the facility passes through an air filter between a zone containing infectious individuals and a zone containing susceptible individuals [96, 100]. This is handled by defining the filter in a zone

$$\frac{dC_i(t)}{dt} = -Q_{ri}\eta_{ri}C_i(t) \quad , \tag{3.13}$$

where η_r is the efficiency of the filter at removing the pathogen from the circulated air Q_r passing through the filter.

Air filtration was not investigated in the experiment at the AIR facility that will be discussed in the next section; however, this mechanism is still mentioned here for completeness.

3.2.7 Removal of infectious airborne particles using GUV lights

The removal of infectious particles due to germicidal ultraviolet (GUV) irradiation will be assumed manifested as an exponential decay of the bacteria, with none of the bacteria being resistant to the irradiation [96, 100, 106, 107]. This is then modelled as

$$\frac{dC_i(t)}{dt} = -k_i H_i C_i(t) \quad , \tag{3.14}$$

where k_i is the standard decay rate constant due to GUV light for the microbe considered and H_i is the UV fluence ($\mu W \cdot cm^{-2}$) of the fixture [106]. The range of the standard decay rate constant k ($m^2 J^{-1}$) for *M. tuberculosis* is between $0.0987 - 0.4721 m^2 J^{-1}$ [108, 109].

Upper room GUV irradiation can be included in the model in two different ways. The first is to define a separate zone in which the GUV irradiation acts in a room with a transfer of infectious particles between the upper and lower room, based on the air mixing. The second method is to model the upper room GUV irradiation as affecting only a fraction of the zone, with the air being assumed to be well-mixed in this zone. This changes the mathematical expression of (3.14) to

$$\frac{dC_i(t)}{dt} = -\frac{V_{iU}}{V_i} k_i H_i C_i(t) \quad , \tag{3.15}$$

where V_{iU} is assumed to be the volume of the part of the zone i that is exposed to the ultraviolet germicidal irradiation.

The ultraviolet fluence is a function of time if the fluence changes, for example if the GUV lamps are switched on and off on alternating days.

3.2.8 Modelling assumptions

This model serves only to capture the risk of transmission and would thus need to be considered within the framework of a greater epidemiological model if long time frames that investigate airborne disease epidemics is to be considered.

This modelling framework assumes that the quanta that has been expelled as aerosoled droplets stay in the zone unless they are specifically removed through the usage of dynamics that determine this in the designed model.

The unit of time that is chosen for the modelling is not as important as that it is consistently applied in all parameters' unit definitions.

CHAPTER 4 AIRBORNE INFECTIONS RESEARCH FACILITY MODEL AND SIMULATION

4.1 CHAPTER OVERVIEW

As an example of how the modelling framework from Chapter 3 can be used, a model will be developed for the Airborne Infections Research (AIR) facility at eMalahleni (formerly known as Witbank), Mpumalanga [70, 110, 111]. Experimental data that was obtained from a study, on the effectiveness of upper room ultraviolet irradiation (GUV) irradiation, conducted at the AIR facility, are then compared to model predictions. The study at the AIR facility was run from 31 August 2015 to 4 December 2015.

4.2 EMALAHLENI AIR FACILITY MODEL

The Airborne Infections Research (AIR) facility in eMalahleni is alongside the Mpumalanga provincial multidrug-resistant (MDR) tuberculosis referral hospital, and is used to conduct experiments on the efficacy of different interventions aimed at reducing TB transmission, and in particular MDR tuberculosis transmission. These interventions included upper room GUV irradiation, surgical face masks used by TB patients, and portable room air disinfection units.

The AIR facility consists of wards for TB patients and two animal rooms, and is based on the design of the research facility used by Riley from 1958-1962 [74]. The wards consist of three rooms, with two beds in each room, patient ablutions and a patient day room. A maximum of six patients can be accommodated in the AIR facility. A layout of the ward area and the patient rooms is shown in Figure 4.1.

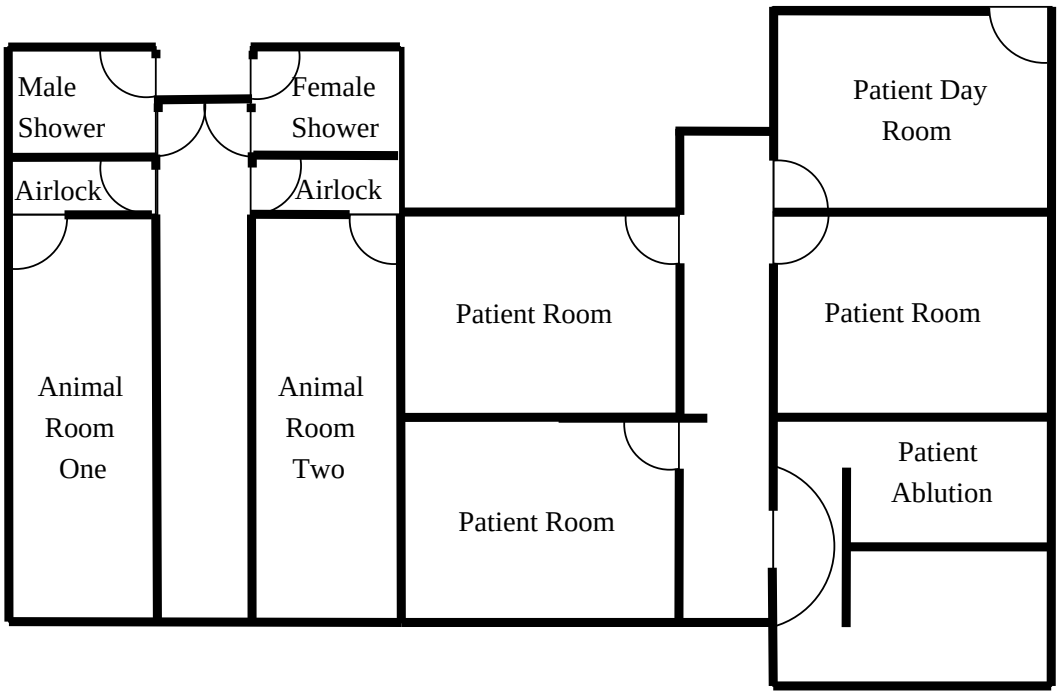

Figure 4.1. The layout of the wards and animal rooms of the Airborne Infections Research (AIR) facility in eMalahleni.

The assumption in the model will be made that the air is well-mixed because there are paddle fans in each of the ward rooms to help facilitate the air mixing in the room. The air turnover rate, or air changes per hour ($AC \cdot h^{-1}$), of the paddle fans used in the AIR facility is approximately 57 $AC \cdot h^{-1}$ [111]. This is much greater than the ventilation rate, which was estimated to be between 3-6 $AC \cdot h^{-1}$. This means that for each air change that occurs, the air in the room is circulated approximately 10 times. Using these paddle fans, the assumption of well-mixed air seems reasonable. Otherwise a zonal model can be expanded to conform to imperfect air-mixing [94].

The facility is described by two sets of susceptible populations $S_x(t)$, representing the guinea pigs in each animal room and a single population of infectious individuals $I_w(t)$. Three zones are considered in this model. The first zone considered is the ward $i = w$, which consists of the three rooms, common room and toilets where the infectious patients stay. The other two zones considered are the spaces occupied by the cages in each of the two animal rooms; $i = 1$ for animal room one and $i = 2$ for animal room two. Since the guinea pigs only have access to the space their cage occupies, only this space will be considered as a zone. The volume considered in each of these zones is given by V_i. There are no paddle fans in the animal rooms, therefore the air the guinea pigs are exposed to is only moved

through the ventilation system. However, the inlet ventilation air into the animal rooms is split up and delivered through an installed diffuser in front of each of the cages. This system ensures that the sentinel animals, in their cages, are each exposed to approximately equal amounts of ventilation air, as well as having good airflow over each cage space.

Nine state variables are used to describe the AIR facility. Three states describe the number of infectious particles in each of the three zones $C_i(t)$. Six states describe the guinea pig populations; three for each animal room: $x = 1$ for animal room one and $x = 2$ for animal room two. The guinea pig population is described through classification as infected $I_x(t)$, exposed $E_x(t)$ or susceptible $S_x(t)$. The model is given in (4.1)-(4.9).

$$\frac{dS_1(t)}{dt} = -p\theta\frac{C_1(t)}{V_1}S_1(t) \tag{4.1}$$

$$\frac{dS_2(t)}{dt} = -p\theta\frac{C_2(t)}{V_2}S_2(t) \tag{4.2}$$

$$\frac{dE_1(t)}{dt} = p\theta\frac{C_1(t)}{V_1}S_1(t) - \alpha E_1(t) \tag{4.3}$$

$$\frac{dE_2(t)}{dt} = p\theta\frac{C_2(t)}{V_2}S_2(t) - \alpha E_2(t) \tag{4.4}$$

$$\frac{dI_1(t)}{dt} = \alpha E_1(t) \tag{4.5}$$

$$\frac{dI_2(t)}{dt} = \alpha E_2(t) \tag{4.6}$$

$$\frac{dC_w(t)}{dt} = \phi_w I_w - \frac{Q_w}{V_w}C_w(t) - k_w H_w\frac{V_{wU}}{V_w}C_w(t) \tag{4.7}$$

$$\frac{dC_1(t)}{dt} = \frac{Q_{1in}}{V_w}C_w(t) - \frac{Q_{1out}}{V_1}C_1(t) \tag{4.8}$$

$$\frac{dC_2(t)}{dt} = \frac{Q_{2in}}{V_w}C_w(t) - \frac{Q_{2out}}{V_2}C_2(t) \tag{4.9}$$

Patients, as the source of the infectious particles I_w, are recruited for the study, based on referral by the adjoining multi drug-resistant tuberculosis hospital. Only individuals with lab confirmed positive acid-fast bacilli (AFB) sputum smear test results are considered for inclusion in the study. The patients are intended to remain at the AIR facility for two weeks. They are required to spend at least 20 hours a day within the facility, although most spend more than this due to their illness. The timeline of the patients admitted at the AIR facility for the study is given in Figure 4.2. It will be assumed that the generation of quanta is representative of an average, constant value ϕ_w for all infected individuals.

By using the theoretical quanta of infection, the uncertainty of a number of factors can be lumped into

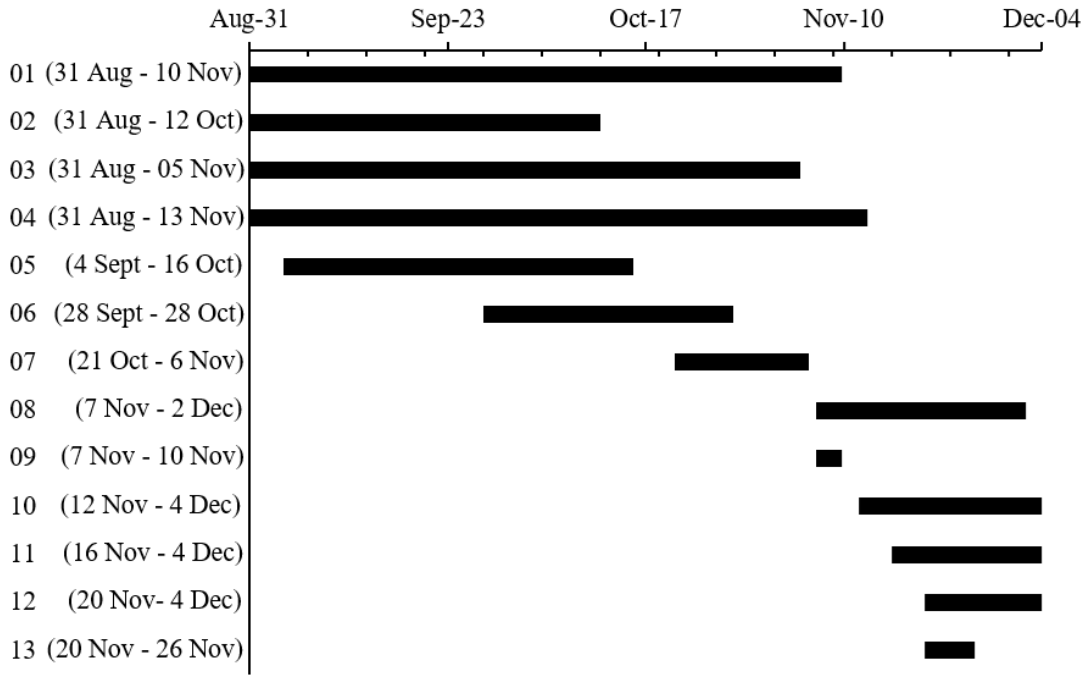

Figure 4.2. The timeline for the patients admitted to the AIR facility and the duration of their admittance. On the y-axis is the patient number. (Patient names are excluded for confidentiality.)

the variable ϕ, allowing for easier estimation of this parameter in the face of uncertainty. The quanta of infection does not, however, give a realistic indication of the number of infectious particles in a zone, but was chosen, instead of a dose response model, because of the problem of a lack of infectious dose data for infections in humans [17].

Each animal room contained 90 guinea pigs, which served as a sentinel animal model for the risk of airborne transmission of TB. Outbred, specific pathogen free, Dunkin-Hartley guinea pigs were used in the experiment, with an equal number being male and female. Two guinea pigs are kept in a cage, but each animal room has 50 cages, leaving 10 cages unused per animal room. It is assumed that all the guinea pigs have the same constant average pulmonary respiratory rate $p = p_1 = p_2$ and that they are equally susceptible to infection $\theta = \theta_1 = \theta_2$. The incubation period of the pathogen is given by $\alpha = \alpha_1 = \alpha_2$, the time taken from infection until the guinea pig exhibits symptoms of infection or reacts positively to tuberculin skin test (TST) diagnosis. Infected animals are euthanised and not replaced during the course of an experiment. Animal care was overseen by a licensed laboratory veterinarian and all protocols were approved by the Animal Use committees of the South African MRC, the US CDC, and Harvard Medical School.

The ventilation system airflow out of the wards Q_w is routed to either of the two animal rooms. The animal rooms receive ventilation air from either the patient ward Q_{iin} or high efficiency particulate arrestance (HEPA) filtered outside air on alternate days. The ward air is assumed to be contaminated with the pathogen, and HEPA filtered outside air is assumed to be pathogen-free. The animal room ventilation is such that when animal room one receives ward air, animal room two will receive HEPA filtered outside air. The airflow out of the animal rooms Q_{iout} is assumed to be equal to the combined airflow into an animal room. This assumption is made because no direct measurement for the airflow rate out of the animal rooms is available; however the airflow out is controlled to maintain a constant negative pressure in the animal rooms.

On the days that animal room one receives the ward air, upper room GUV lights are turned on inside the wards. The fluence of the UV light fixtures H_w is then either equal to the output fluence of the fixture or zero, depending on whether the GUV fixtures are on or off. The standard decay rate constant due to GUV irradiation for *M. tuberculosis* is given by k_w. Animal room two is assumed to be the control room for this experiment, aimed at determining the efficacy of upper room GUV light, and receives ventilation air untreated by GUV lights.

The two animal rooms in the facility are maintained under animal biosafety level 3 conditions [112]. The temperature in the animal rooms is kept at $22 \pm 1°C$, with a relative humidity of $50 \pm 10\%$. Workers are required to wear a 3M 6000 full face respirator. It can therefore be assumed that the only source of infection of the guinea pigs is from the air from the patients through the ventilation system. Additionally, the workers must shower before entering and upon exiting the animal room area. The showers and airlocks are indicated in Figure 4.1.

The model for the AIR facility, given by (4.1) to (4.9) has been solved in Addendum A. This has been done to provide an alternative to using numerical integration to simulate using the model. However, in this text the simulations are done using numerical integration.

4.3 GERMICIDAL ULTRAVIOLET IRRADIATION STUDY

The AIR facility study that ran from 31 August 2015 to 4 December 2015 will be simulated using the model given by (4.1) - (4.9). The simulation is performed by solving the model using the Runga-Kutta integration method with a fixed time step of 1 minute per time step [113, 114]. The parameters required

to solve the model are obtained from a variety of sources. The ward, duct and animal cage dimensions are obtained from measurements at the facility and given in Table 4.1.

The ventilation rates, the GUV fixture fluence and the infectious source are taken as time varying parameters to accommodate the study situation. The ventilation data and the GUV fixture switching are obtained from the Supervisory Control and Data Acquisition (SCADA) system installed in the AIR facility. This gives a real-time measurement of the airflow rates between the different zones of the facility. The ventilation airflow rate data from the SCADA system for the airflow out of the ward is given in Figure 4.3 and the measured airflow into and out of the two animal rooms is given in Figure 4.4.

Table 4.1. The measured parameters from the AIR facility used for the simulation. The parameters are defined in their most convenient units.

Measurement	Value
$A_{duct:ward\,out}$	$0.09m^2$
$A_{duct:ward-animal\,room}$	$0.015m^2$
$A_{duct:animal\,room\,clean\,air}$	$0.034m^2$
N_{cage}	50
$V_{ward\,room\,1}$	$3.0m \times 4.8m \times 2.6m$
$V_{ward\,room\,2}$	$3.2m \times 4.8m \times 2.6m$
$V_{ward\,room\,3}$	$2.9m \times 4.8m \times 2.6m$
$V_{ward\,common\,room}$	$5m \times 4m \times 2.6m$
V_{cage}	$0.56m \times 0.35m \times 0.36m$
V_w	$164.8m^3$
V_{Uw}	$21.7m^3$
V_{a1}	$174.8m^3$
V_{a2}	$174.8m^3$

The upper room GUV fixture fluence is 5 $\mu W \cdot cm^{-2}$ when it is on [111], and the fluence is taken as zero when it is off. The GUV light is assumed to uniformly irradiate the space in the patient ward above a height of 2.1 m, or a volume of $V_{wU} = 21.7\ m^3$. The on and off switching data is obtained from the SCADA system, and the resulting GUV fluence in the ward is shown in Figure 4.5.

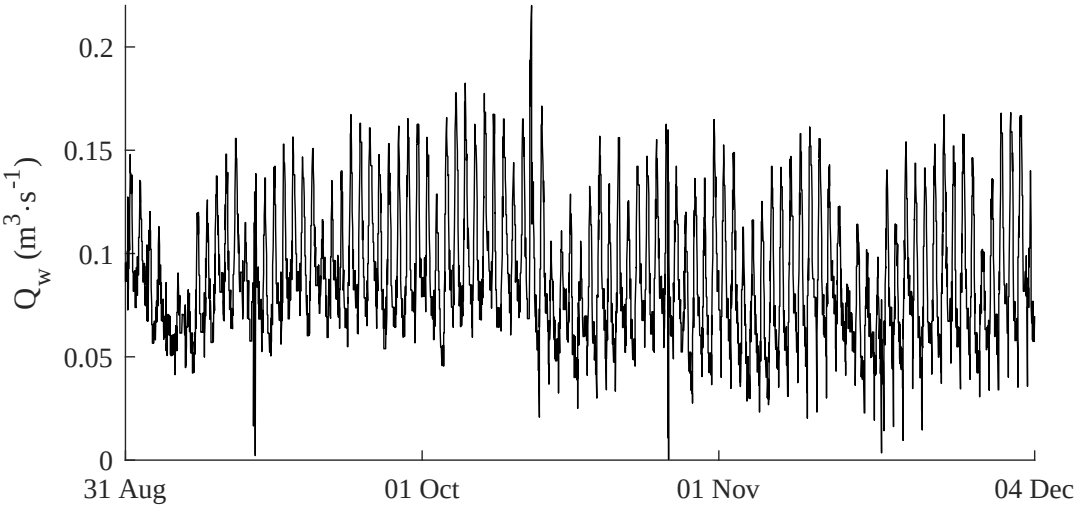

Figure 4.3. The volumetric air flow rate from the patient wards to the animal rooms, which is calculated by taking the measured SCADA system values in $(m \cdot s^{-1})$ and multiplied by the area of the duct.

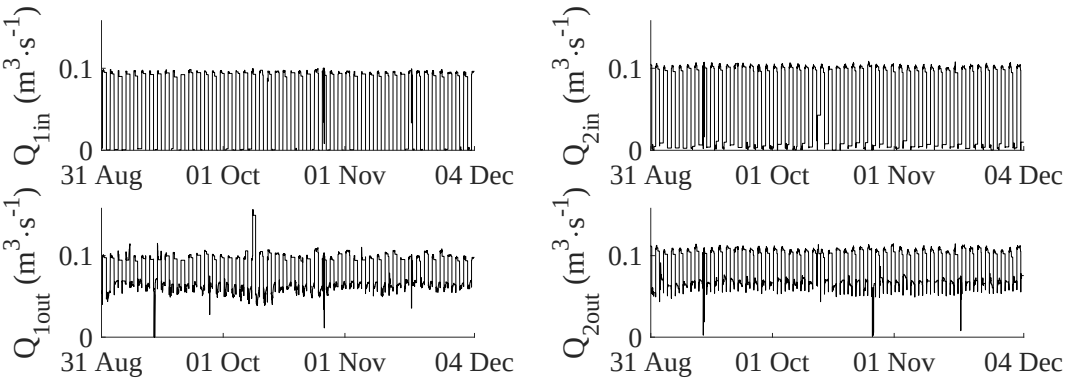

(a) Animal room one

(b) Animal room two

Figure 4.4. The volumetric air flow rates into the animal rooms Q_{xin} (top) are calculated by taking the measured SCADA system airflow velocity $(m \cdot s^{-1})$ and multiplied by the area of the duct. The volumetric air flow rates out of the animal rooms Q_{xout} (bottom) are calculated by taking the ward air flow rate Q_{xin} and adding the measurement of the HEPA filtered air flow rate into the animal room.

The infectious source parameter I_w is defined by the number of patients at the AIR facility and is obtained from the patient timeline, Figure 4.2. Patients are arbitrarily assumed to enter and leave the AIR facility at the start of a work day, which is taken to be at 6 AM. The number of patients in the wards for each day of the study is shown in Figure 4.6.

The exact time of day that new patients are being admitted and patients are being discharged is not known. The assumption that patients only enter and leave the facility at 6 AM is chosen, because it simplifies the timing for the purpose of the simulation. This is also the time that was set for the automatic switching of the ward air from one animal room to the other by the SCADA system.

The remaining model parameters needed for the simulation are taken from literature. The source of these parameters is given in Table 4.2, along with the literature reference. Where the given parameters in Table 4.2 are ranges, the actual value used for the simulation still needs to be determined. For this simulation, the GUV irradiation decay constant is chosen to be the lowest value of its range, $k_w = 0.0987$.

Table 4.2. The parameters used for the simulation and their source. The parameters are defined in their most convenient units.

Parameter	Value	Source
ϕ	1.25 - 12.7 $quanta \cdot h^{-1}$	[99]
p	0.23 $m^3 \cdot h^{-1}$	[66]
θ	1 $quanta^{-1}$	[17]
α	0.03 - 0.2 day^{-1}	[115]
k	0.0987 - 0.4721 $m^2 \cdot J^{-1}$	[106]
H	5 $\mu W \cdot cm^{-2}$	[111]

4.4 STUDY PARAMETER ESTIMATION

Due to the range of the quanta generation rate, ϕ_w, and the incubation period, α, that is given within the literature, a parameter estimation problem is set up. This is to estimate the parameter values within the ranges given in Table 4.2 that best fit the data obtained from the AIR facility.

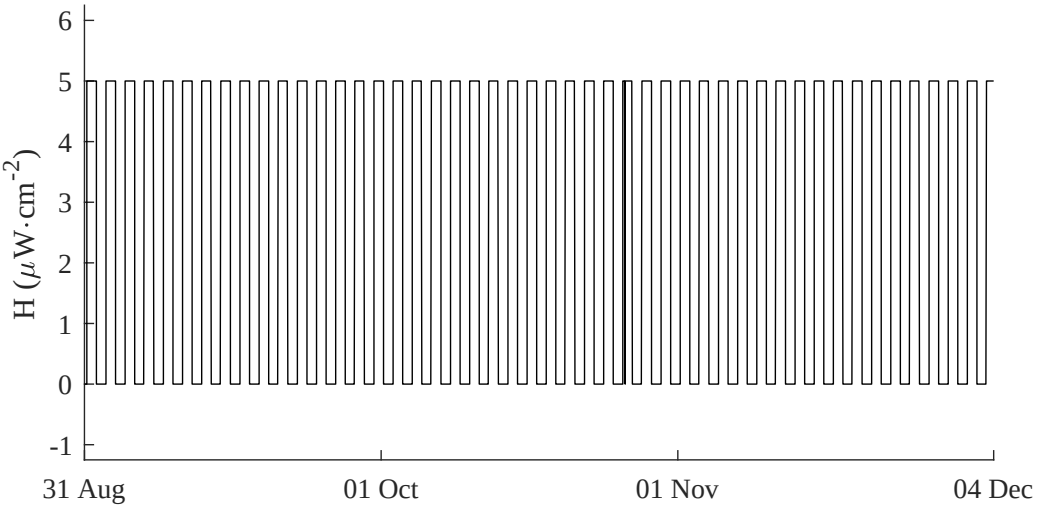

Figure 4.5. The upper room GUV fixture fluence H in the AIR facility. The GUV lamps were switched on during the days animal room one received ward air and were switched off during the days animal room two received ward air.

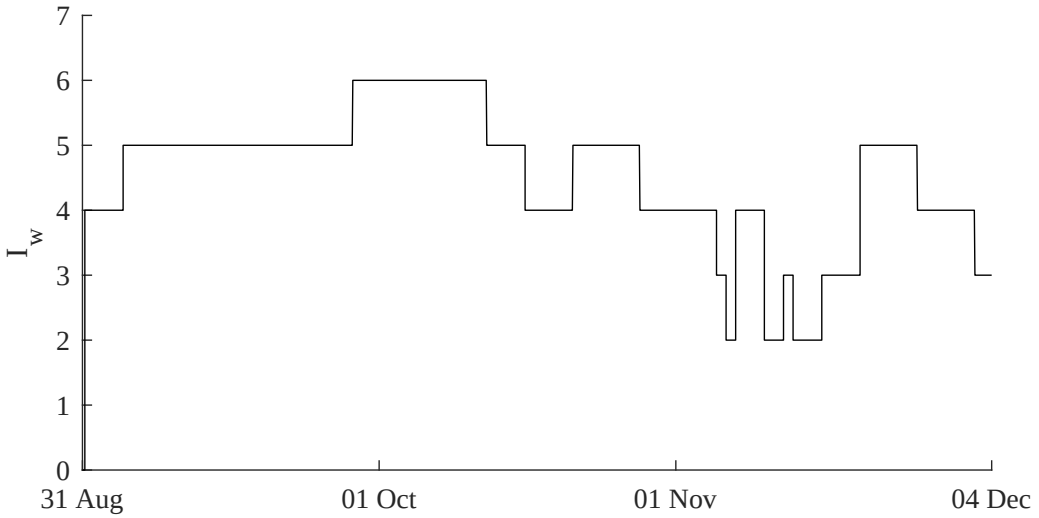

Figure 4.6. The total number of patients in the wards during each day of the experiment. All of these patients are assumed to expel infectious particles at the same hourly rate.

A least squares, cost function minimisation approach is used in the parameter estimation [89]. This method involves the minimisation function solving the model given by (4.1) - (4.9) for a set of ϕ_w and α chosen by the minimisation function, then evaluating the cost of the solution. Through an iterative process, the minimisation function chooses a set of ϕ_w and α to minimise the cost.

The minimisation cost function is set up to be

$$\begin{aligned} J(\alpha,\phi) = & \sum_{j=1,2,3} (I_1(t_j) - I_{1,j})^2 \\ & + \sum_{j=1,2,3} (I_2(t_j) - I_{2,j})^2 \\ & + R \cdot (\mathcal{H}(\alpha - \alpha_{max}) \cdot (\alpha - \alpha_{max})^2 \\ & + \mathcal{H}(\alpha_{min} - \alpha) \cdot (\alpha_{min} - \alpha)^2 \\ & + \mathcal{H}(\phi - \phi_{max}) \cdot (\phi - \phi_{max})^2 \\ & + \mathcal{H}(\phi_{min} - \phi) \cdot (\phi_{min} - \phi)^2) \end{aligned} \tag{4.10}$$

The cost function's first term describes the error between the simulation output, $I_x(t_j)$, and the TST results, $I_{x,j}$, of the number of infected in each animal room, x, for each of the TST measurements, j. The Heaviside function, $\mathcal{H}$, is used to penalise solutions that fall outside of the range allowed for the parameters, as given in Table 4.2. The tuning factor, R, is used to penalise a solution that lies outside the constraint range more than the error between the simulation output and TST results. The tuning factor is set to $R = 100$, ensuring that the minimisation function does not violate the given parameter ranges from Table 4.2.

The Nelder-Mead simplex search function is used as a derivative-free based minimisation algorithm for this problem [116]. The quanta generation rate for the simulations is found to be $\phi_w = 2.5$ and the incubation period is $\alpha = 0.03$. This was found with a final minimisation cost function value of $J = 300$. The root mean square error (RMSE) is 13.48 .

The parameters units with a time aspect are all scaled in the simulation so that all the units and the integration time step match up. Although this is an obvious step, it is important to remember for the validity of the simulation results. Additionally, the initial conditions used for the simulation are given in Table 4.3.

The solution of the model, for each iteration of the minimisation function, is obtained using the Runga-Kutta integration method with a fixed time step of 1 minute per time step [113, 114].

The simulation results, of the 31 August 2015 to 4 December 2015 experiment at the AIR facility, are given in Figure 4.7, for the state variables of the guinea pig infected, exposed and susceptible populations for each of the animal rooms and the number of infectious particles in each of the three zones. The TST results of Table 4.4, that fall within the period of the simulation, are also incorporated into Figure 4.7.

If the parameter estimation is again performed in the unbounded scenario, then the new values for the quanta generations rate is $\phi_w = 61.5$ and for the incubation period is $\alpha = 0.0027$. This gives only a slightly better RMSE of 11.02. Preference is therefore given to the literature bound viable results.

Table 4.3. The initial conditions used for the simulation.

Initial condition	Value
$S_1(t_0)$	90
$S_2(t_0)$	90
$C_w(t_0)$	0
$C_1(t_0)$	0
$C_2(t_0)$	0
$I_1(t_0)$	0
$I_2(t_0)$	0
$E_1(t_0)$	0
$E_2(t_0)$	0

Table 4.4. Tuberculin skin test results for the two animal rooms. The total considered to have been infected per animal room is given by the sum of the number with positive TST results and the number euthanised.

	20 Aug 2015	01 Oct 2015	30 Oct 2015	25 Nov 2015
Animal room 1 positive TST:	0	0	9	11
Animal room 1 euthanised:	0	0	0	11
Animal room 1 total infected:	0	0	9	22
Animal room 2 positive TST:	0	0	2	5
Animal room 2 euthanised:	0	0	0	14
Animal room 2 total infected:	0	0	2	19

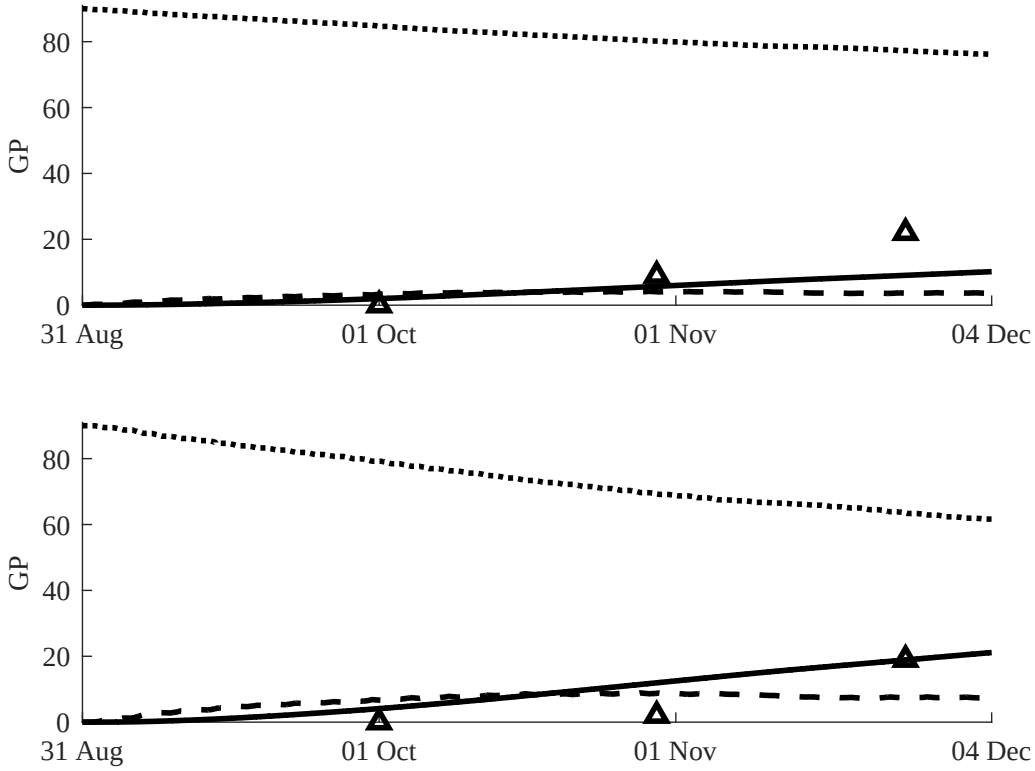

Figure 4.7. The infected (solid), exposed (dashed) and susceptible (dotted) guinea pig (GP) populations in the AIR facility. The animal room one guinea pig populations (top) receive ward air during days when the upper room GUV fixtures are on, and animal room two guinea pig populations (bottom) receive ward air during the days when the upper room GUV fixtures are off. The total number of infected guinea pigs that were observed during the experiment (triangle), and as given in Table 4.4.

CHAPTER 5 RESULTS AND DISCUSSION

5.1 CHAPTER OVERVIEW

The simulation results, of the 31 August 2015 to 4 December 2015 experiment at the AIR facility, are given in Figure 4.7 and Figure 5.2, for the state variables of the guinea pig infected, exposed and susceptible populations for each of the animal rooms and the number of infectious particles in each of the three zones. The TST results of Figure 4.4, that fall within the period of the simulation, are also incorporated into Figure 4.7.

5.2 GUINEA PIG POPULATION SIMULATION RESULTS

The TST results are taken as the measure of the number of infected guinea pigs. As an animal model, the guinea pig has a similar disease progression as a result of infection by the *M. tuberculosis* pathogen as that of humans, albeit synonymous to the response of the unsuccessful immune response of a human [65, 117]. This makes guinea pigs well suited for airborne *M. tuberculosis* transmission studies as sentinel animals [118]. However, this measure of infectiousness is problematic, because it does not account for the complexity and dynamics of disease manifestation in the guinea pig.

The exposed guinea pig population is an unmeasured state that attempts to account for some of the disease manifestation complexities and dynamics by introducing an incubation period. This is an attempt at modelling the delay between infection by the pathogen to diagnosis through a visible induration from a TST. However, the exposed guinea pig population result is theoretical, and should be considered with care; reversions [70], for instance, have also not been included in the model.

The difference between the simulated number of infected guinea pigs and the experimental results (that is, the difference between solid line and triangles in Figure 4.7) is shown in Figure 5.1. It can

be seen that the simulated animal room one infected population better reproduces the experimental measurement of infected animals initially, but the simulated animal room two infected population is a much better fit for the end of the experiment.

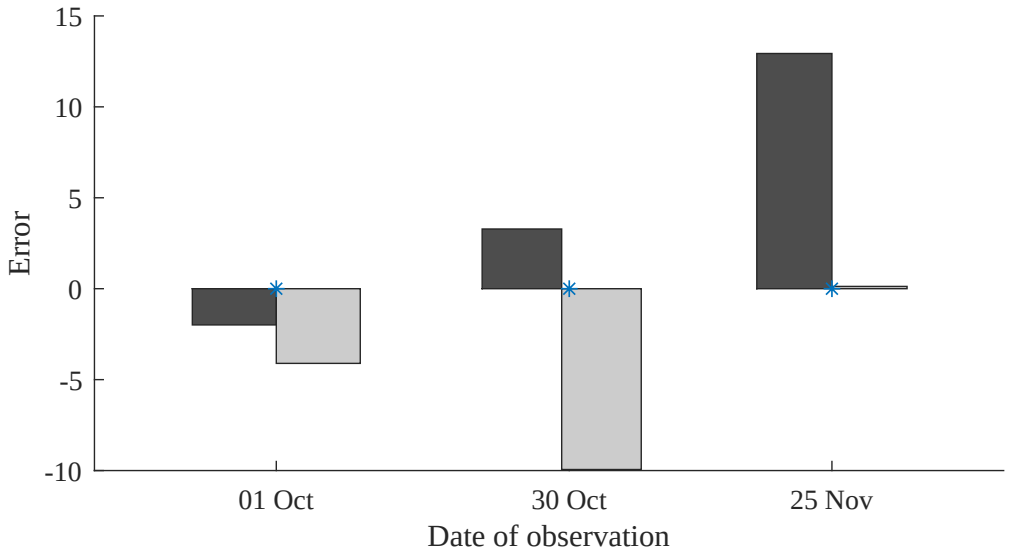

Figure 5.1. The error of the prediction giving the difference between the number of infected from the experiment and the simulated results. The left bars indicate the difference for animal room one, and the right bars for animal room two.

5.3 INFECTIOUS PARTICLE SIMULATION RESULTS

The number of infectious particles in the zones is an unmeasured, 'internal' state of the model. These states account for higher order dynamics in the prediction of the infected population, but their absolute value is theoretical, and should be considered as such. The unmeasured states of the quanta of infectious particles in the three zones is shown in Figure 5.2, and an arbitrary two day period is shown in Figure 5.3 to show the day to day pattern. Considerable fluctuations in the number of quanta in the zones can be noted from Figure 5.2, with three mechanisms attributed as responsible for these fluctuations.

The first mechanism that impacts the fluctuations in the number of infectious particles is the number of patients in the wards. This is clear from (4.7); however, it can also be seen when comparing Figure 4.2 and 5.2. As an example, the average number of number of quanta on a day when the GUV lights are on can be compared during the first few days in October versus middle November. On 2 October 2015, six patients are in the ward and the average number of quanta is 3.8; however, on 15 November 2015,

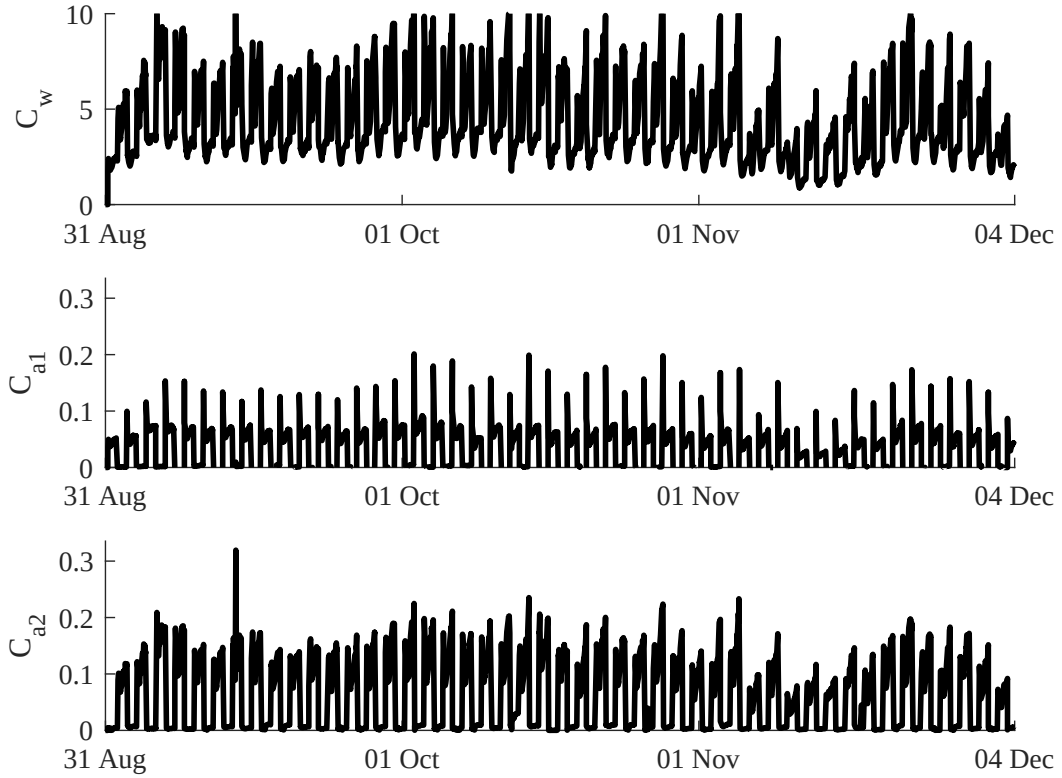

Figure 5.2. The number of quanta C_w (patient wards), C_{a1} (animal room one) and C_{a2} (animal room two) in each of the zones considered for the AIR facility.

only two patients are in the ward and the average number of quanta is 1.4. The average airflow out of the ward is similar on the two days, being 0.0793 $m^3 \cdot s^{-1}$ on 2 October 2015 and 0.0674 $m^3 \cdot s^{-1}$ on 15 November 2015.

The second mechanism that impacts the fluctuations of infectious particles in the zones is the ventilation rate. For the two animal rooms (Figure 4.4) this is expected to have a big impact on the fluctuations, because of the switching between ward air and clean HEPA filtered outside air on alternate days. When no ward air is supplied to the respective animal room, there is no source of infectious particles, and the clean air supply quickly removes the infectious particles that are in the animal room.

However, not only are the fluctuations of the air flow rate into the animal rooms significant, but so are the fluctuations in the airflow out of the wards. This airflow fluctuates due to day-night swings in temperature, because the temperature feedback controller of the ward outlet fan was run in manual mode. The airflow fluctuation is especially noticeable on the simulated number of infectious particles

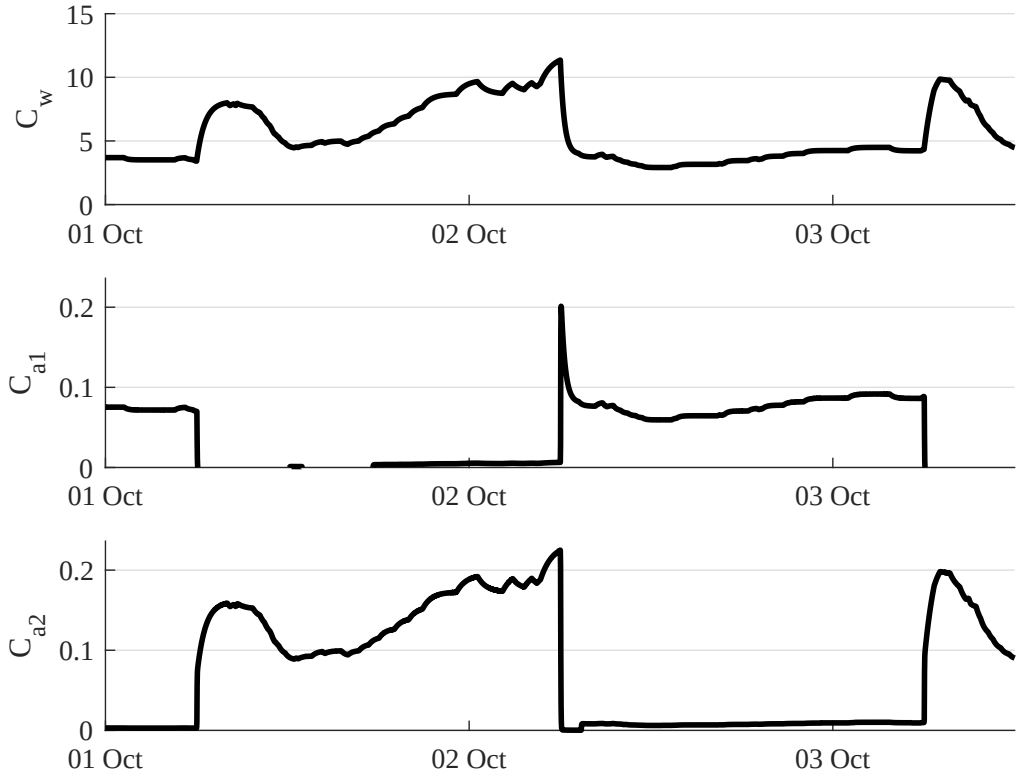

Figure 5.3. The number of quanta C_w (patient wards), C_{a1} (animal room one) and C_{a2} (animal room two) in each of the zones considered for the AIR facility. However, only a two day period is shown to highlight the day to day pattern seen in Figure 5.2.

in animal room two, as seen in Figure 5.3. The facility also experienced a number of power outages, due to an unstable supply from the national South African electrical grid during this period, causing the ventilation (and GUV fixtures) to switch off for the short span of time between the power outage and the time taken before the backup diesel generator switched in.

When the average ward air received by each of the two animal rooms from Figure 4.4 is compared, it is found that animal room one gets 12.7% less ward air than animal room two. The average combined air into the animal rooms is 10.7% higher than the average measured air out of the ward. These deviations are most like a result of inaccuracies with the air flow measurement instruments, and give an idea of the typical uncertainty surrounding these measurements.

The third mechanism that impacts the fluctuations of infectious particles in the zones, is the upper room GUV irradiation. However, this fluctuation is intended from the experiment design. It can be seen

from Figures 5.2 and 5.3 that animal room one receives approximately half the number of infectious particles as opposed to what animal room two receives. This is due to the upper room GUV irradiation lowering the number of infectious particles in the wards on the days when it is on. This then also translates to fewer number of simulated infections in animal room one.

5.4 SENSITIVITY OF THE SIMULATION PARAMETERS

There is significant uncertainty surrounding some of the parameters that were used in the simulation, which is mostly due to the large viable ranges of the parameters obtained from literature. To quantify the uncertainty, two sensitivity analyses were performed on the parameters used in the simulation. Both sensitivity analyses were conducted by keeping all parameters constant, and varying only a single parameter at a time.

The first sensitivity analysis aims to illustrate what the effects of uncertainty in the parameter values taken from literature are. The α, k and ϕ parameters were each varied by their range given in Table 4.2, and the number of patients I_w in the ward each day was increased and decreased by one. The resulting predictions for the number of infected guinea pigs in animal room one and animal room two can be seen in Figure 5.4. From this analysis, the impact of not knowing the true values of α, k and ϕ on the simulation outcomes is demonstrated. However, of greatest concern to the accuracy of simulation results is the quanta generation rate parameter, ϕ, which has the biggest impact on the simulation results for its plausible literature range. From the value used in the simulation, ϕ can vary by 458%, which means the outcome of the simulation (the predicted number of infected guinea pigs) for animal room one can vary by 351% and for animal room two can vary by 256%. However, model parameters that have been obtained through instrumentation measurements by the SCADA system are expected to have low uncertainty (on the order of $1-10\%$ for typical instrumentation [119]).

The second sensitivity analysis aims to illustrate the relative uncertainty in the different model parameters by increasing and decreasing each by an equal amount one parameter at a time. The resulting predictions for the number of infected guinea pigs in animal room one and animal room two, when each parameter was arbitrarily increased and decreased by 50% while keeping the others constant, can be seen in Figure 5.5. From this analysis, it can be seen how the error of the true parameter value and the estimated value would affect the accuracy of the simulation results. It can also be noted that an uncertainty in some parameters is indistinguishable from an uncertainty in others, for example,

the uncertainty in pulmonary respiration rate p, the quanta generation rate ϕ and the susceptibility to infection θ all affect the simulation outcome equally. This means that by estimating the quanta generation rate ϕ, any error between the true and simulated values of the pulmonary respiration rate or susceptibility to infection, would result in a corresponding error between the true and simulated value of the quanta generation rate. Additionally, the airflow Q_{1in} and Q_{1out} have a similar effect on the results, but in different directions, giving the same overall band of uncertainty; Q_{2in} and Q_{2out} affect animal room two instead of animal room one.

The sensitivity of the model to the quanta generation rate parameter, ϕ, indicates a research gap around the quanta of infection. Refining the constituent mechanism of the quanta of infection, can be beneficial in improving the predictability of simulations. This would also improve the understanding of factors that play a role in the mechanism of TB transmission. However, the quanta of infection unit of measure transparently represents this uncertainty, because it is a hypothetical unit. To refine the understanding of transmission and move away from the quanta of infection unit, would require additional measurements or other forms of experimental data [120].

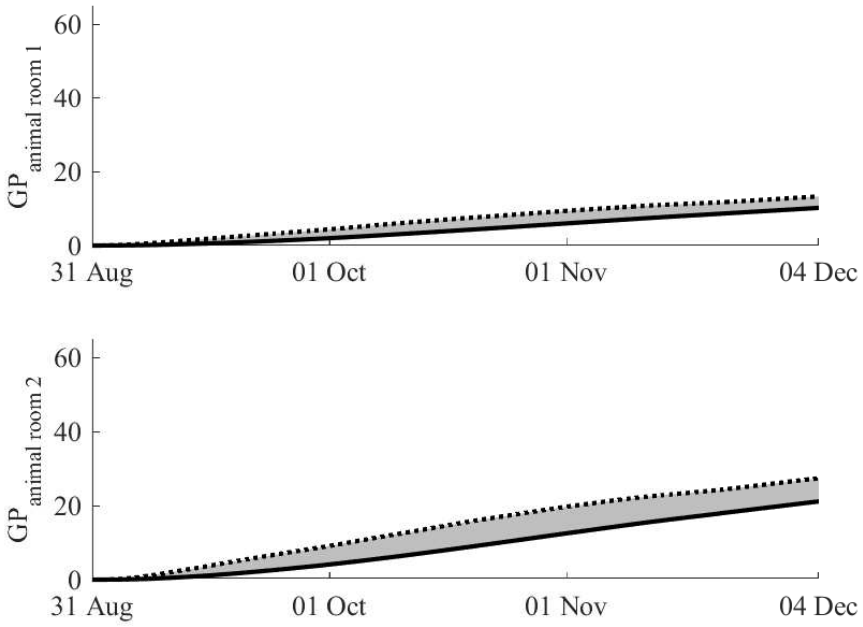

(a) α

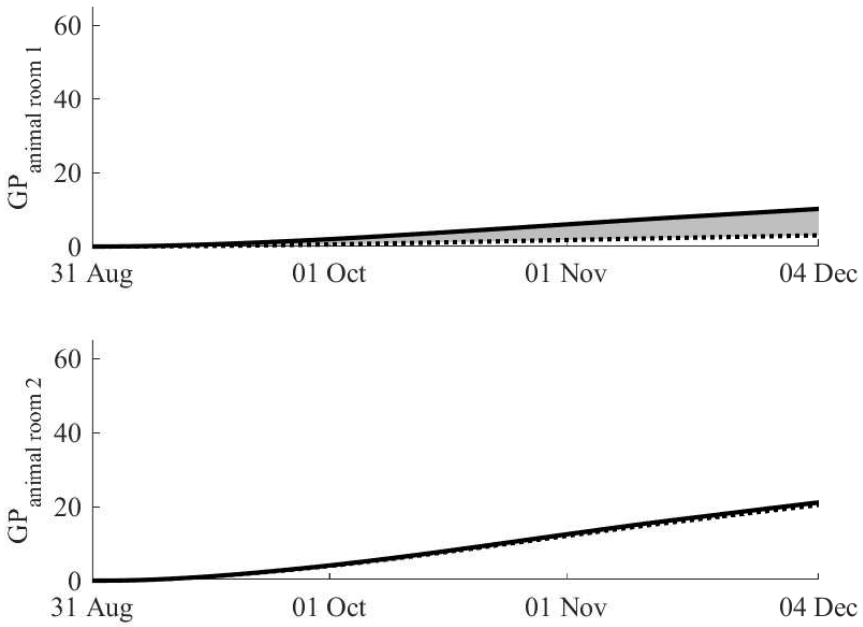

(b) k

Figure 5.4. The sensitivity of the number of infected guinea pigs (GP) when each of the parameters is varied by their literature given range, as in Table 4.2. The black line indicates the simulated number of infected guinea pigs, and the gray area the band of variation. The number of patients in the ward, I_w, was varied by ± 1 patient.

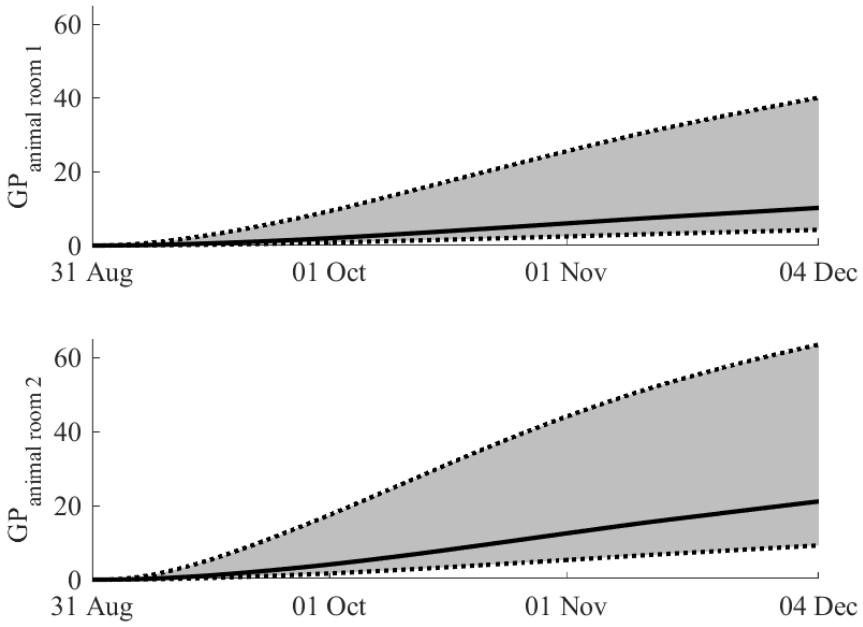

(c) ϕ

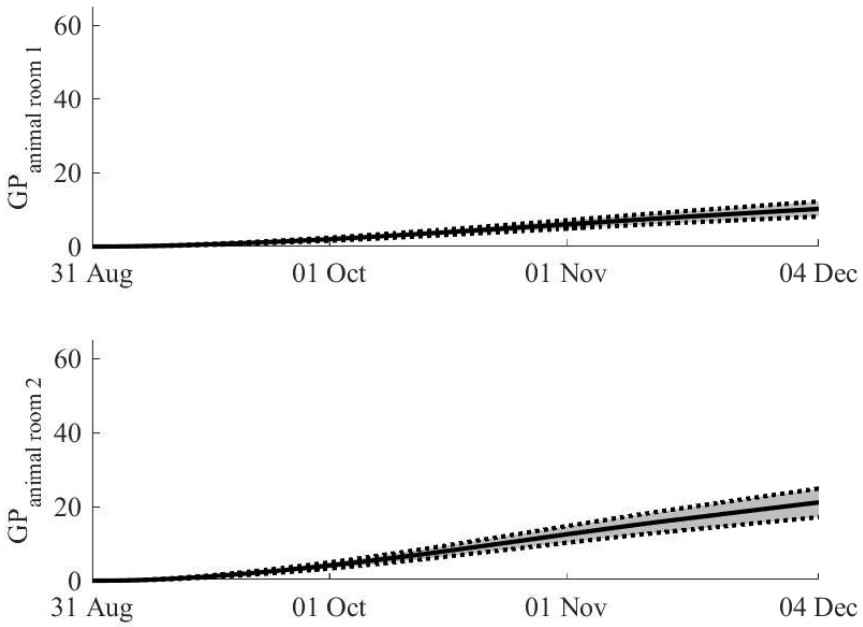

(d) I_w

Figure 5.4. The sensitivity of the number of infected guinea pigs (GP) when each of the parameters is varied by their literature given range, as in Table 4.2. The black line indicates the simulated number of infected guinea pigs, and the gray area the band of variation. The number of patients in the ward, I_w, was varied by ± 1 patient. (Continued.)

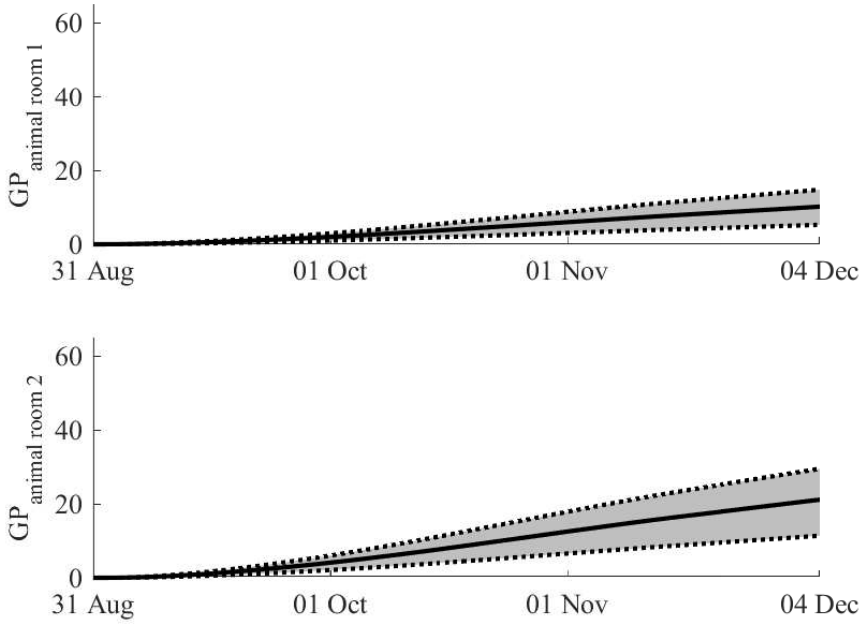

(a) p, ϕ and θ

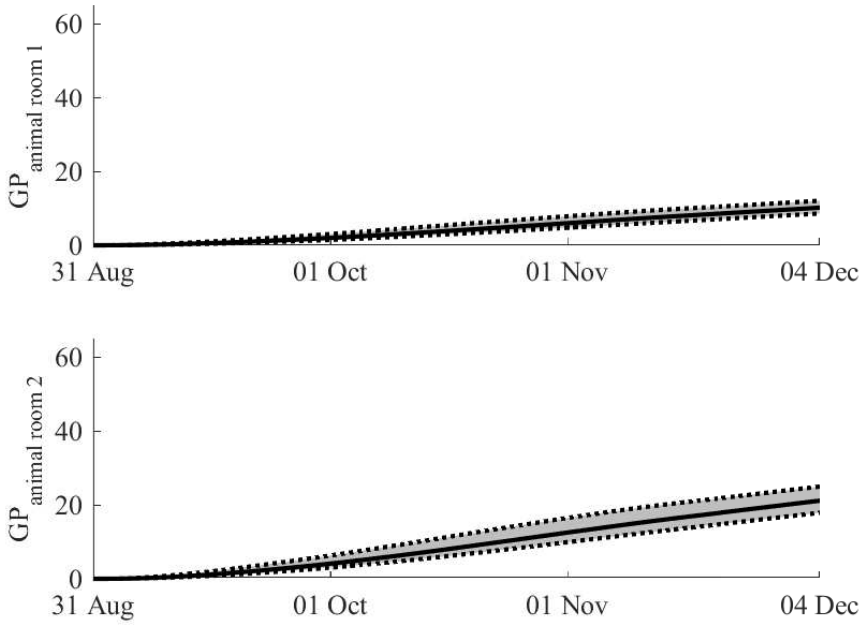

(b) α

Figure 5.5. The sensitivity of the number of infected guinea pigs (GP) when each of the parameters is varied by $\pm 50\%$. The black line indicates the simulated number of infected guinea pigs, and the gray area the band of variation due to varying the parameter.

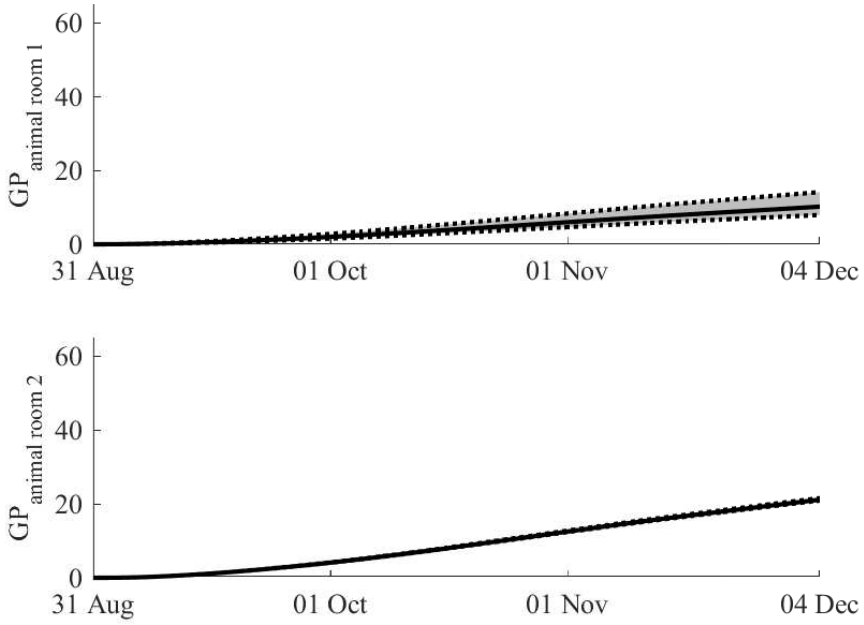

(c) H and k

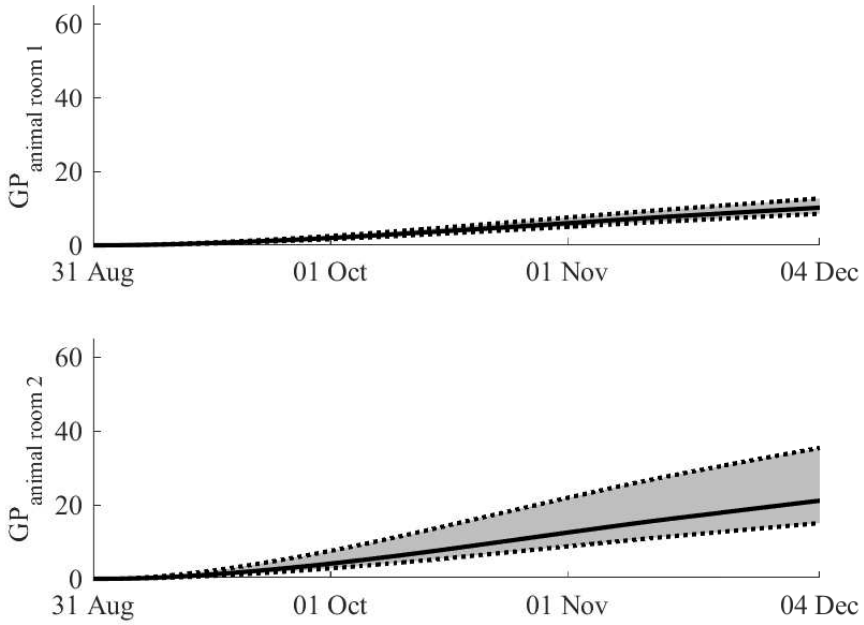

(d) Q_w

Figure 5.5. The sensitivity of the number of infected guinea pigs (GP) when each of the parameters is varied by $\pm 50\%$. The black line indicates the simulated number of infected guinea pigs, and the gray area the band of variation due to varying the parameter. (Continued.)

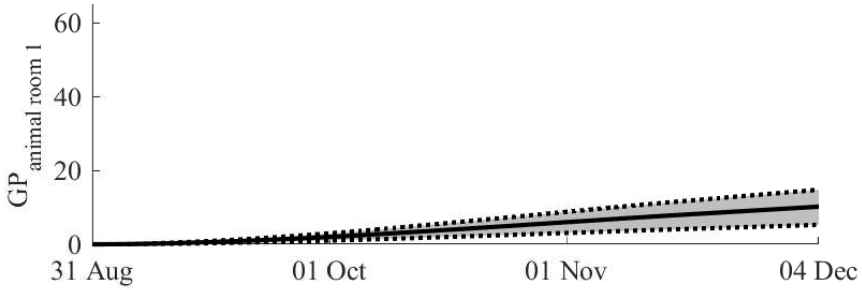

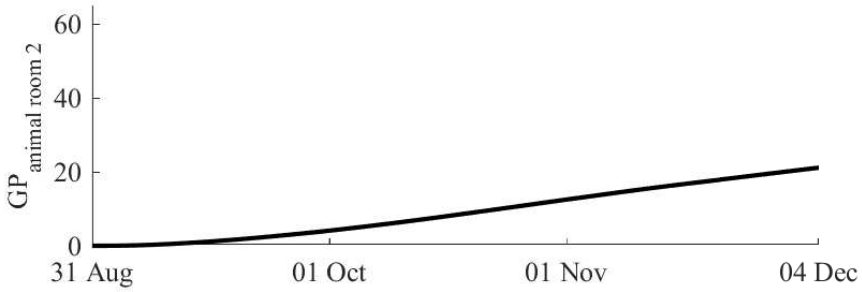

(e) Q_{1in} and Q_{1out}

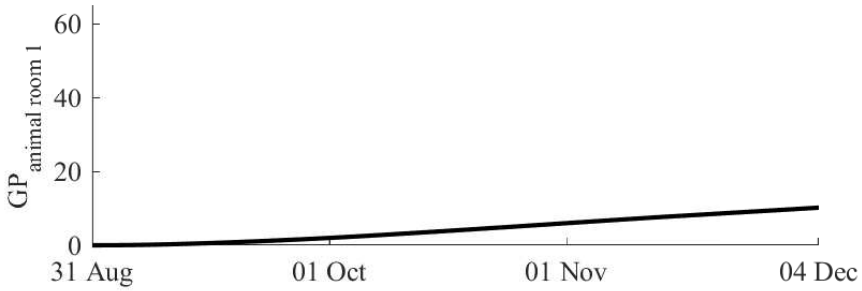

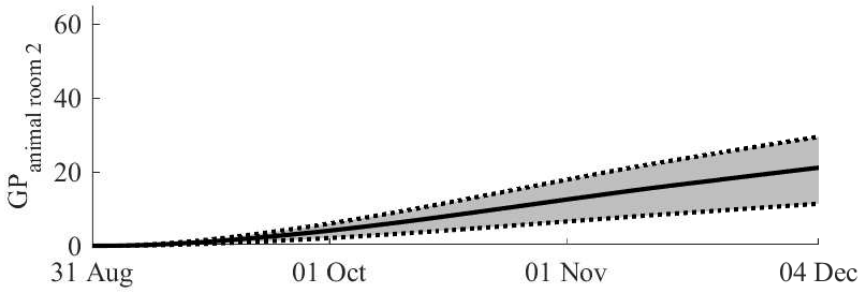

(f) Q_{2in} and Q_{2out}

Figure 5.5. The sensitivity of the number of infected guinea pigs (GP) when each of the parameters is varied by $\pm 50\%$. The black line indicates the simulated number of infected guinea pigs, and the gray area the band of variation due to varying the parameter. (Continued.)

5.5 SUPER-SPREADERS AND THE STUDY

With the study outcome and the simulation, a situation that must be considered is whether one patient in the ward could have caused the majority of the infections. This is along the theory that there are perhaps some people that are more infectious than others when they have active tuberculosis disease. These individuals are then known as 'super-spreaders' [121].

To consider this situation, the average generation of quanta, ϕ_w, is considered as unique for each of the 13 patients, as shown in Figure 4.2. This would then change (4.7) to be:

$$\frac{dC_w(t)}{dt} = \sum_{n=1}^{13}(\phi_{wn}I_{wn}) - \frac{Q_w}{V_w}C_w(t) - k_w H_w \frac{V_{wU}}{V_w}C_w(t) \tag{5.1}$$

The same methodology is then followed for the parameter estimation, again a least squares, cost function minimisation algorithm is used. However, the cost function is now set up to be:

$$\begin{aligned} J(\phi_{n=1,\ldots,13}) = &\sum_{j=1,2,3}(I_1(t_j) - I_{1,j})^2 \\ &+ \sum_{j=1,2,3}(I_2(t_j) - I_{2,j})^2 \\ &+ R \cdot \sum_{n=1}^{13}(\mathcal{H}(\phi_n - \phi_{max}) \cdot (\phi_n - \phi_{max})^2 \\ &\quad + \mathcal{H}(\phi_{min} - \phi_n) \cdot (\phi_{min} - \phi_n)^2) \end{aligned} \tag{5.2}$$

The first term of the cost function describes the error between the simulation output, $I_x(t_j)$, and the TST results, $I_{x,j}$, of the number of infected in each animal room, x, for each of the TST measurements, j. Refer to Section 4.4 for a detailed description of the parameter estimation methodology. The value of $\alpha = 0.03$ is kept from the previous minimisation output, and is not solved again here.

The final minimisation cost function value of $J = 290$ was found, which is slightly lower than the value of 300 when considering the same value of the quanta generation rate ϕ for all the patients. The results of this simulation, with the individual quanta generation rates per patient, are shown in Figure 5.6 and 5.7.

The difference in the results when considering individual patient quanta generation rates (Figure 5.6) and when considering an average infectivity (Figure 4.7) is negligible. However, comparing Figure 5.7

and 5.2, it can be seen that a higher quanta level was expected until the November data point when considering individual patient quanta generation rates.

This simulation indicates that it does not seem as if it was the result of a super-spreader that caused animal room 1 to have higher than expected guinea pig infections.

Table 5.1. The quanta generation rate for each of the patients when solved individually.

Patient	ϕ_{wn}
01	2.5065
02	1.6987
03	2.2434
04	3.4697
05	1.7437
06	2.8572
07	2.7587
08	2.3840
09	0.9989
10	1.9375
11	1.6158
12	1.5696
13	0.9965

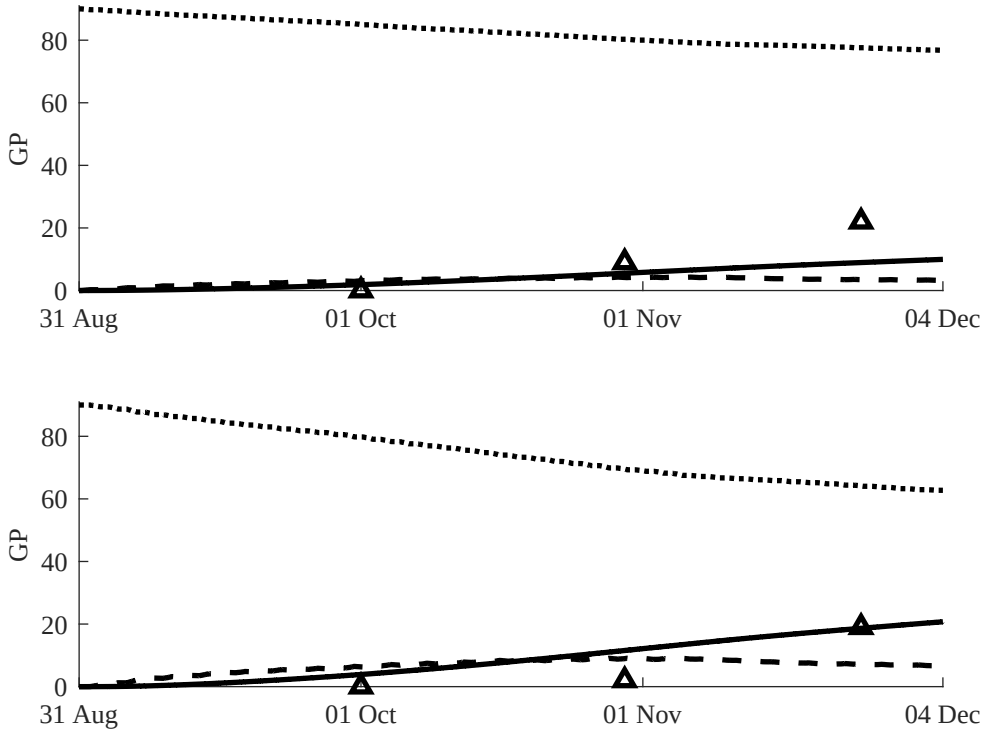

Figure 5.6. The infected (solid), exposed (dashed) and susceptible (dotted) guinea pig (GP) populations in the AIR facility. The animal room one guinea pig populations (top) receive ward air during days when the upper room GUV fixtures are on, and animal room two guinea pig populations (bottom) receive ward air during the days when the upper room GUV fixtures are off. The total number of infected guinea pigs that were observed during the experiment (triangle), and as given in Table 4.4. Simulated for each patient having an unique quanta generation rate.

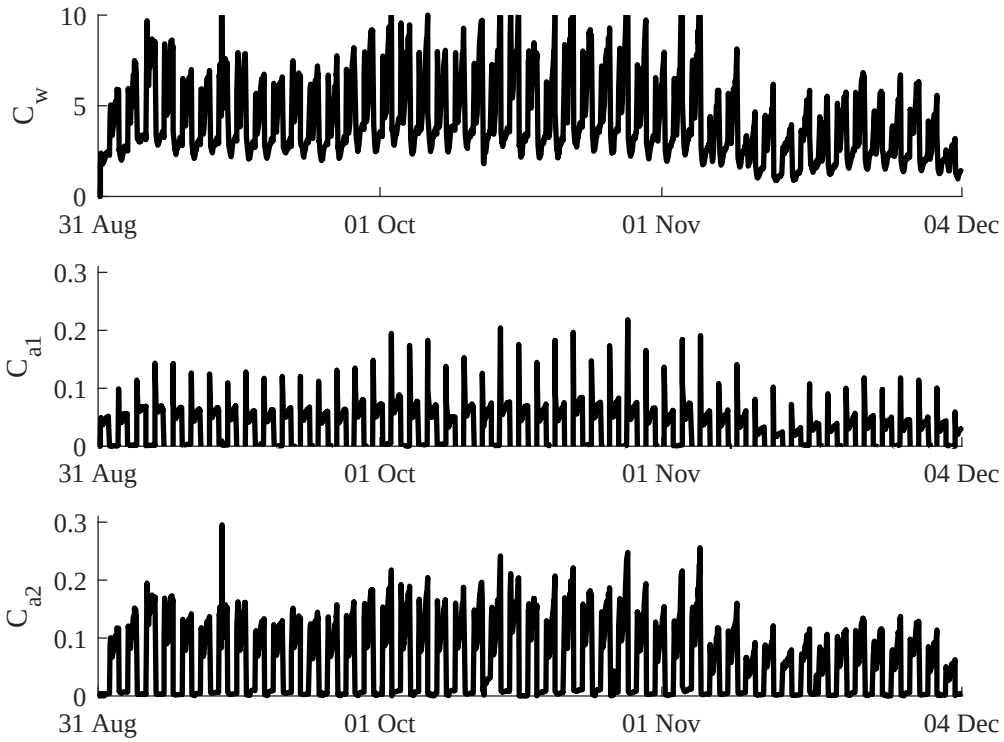

Figure 5.7. The number of quanta C_w (patient wards), C_{a1} (animal room one) and C_{a2} (animal room two) in each of the zones considered for the AIR facility. Simulated for each patient having a unique quanta generation rate.

5.6 SIMULATION FIT AND EXPERIMENT OUTCOME

The major mechanism that influences the difference between the simulated results of the two animal rooms, is the upper room GUV irradiation. Based on the parameters used, the simulation indicates that animal room one should have fewer infections than animal room two. However, animal room one actually had more infections than animal room two. This result is different to what was expected, both from the initiation of the experiment and from the simulation results.

To check whether there was enough contact time of the GUV irradiation with infectious particles, considering the high air turnover rate of $57h^{-1}$ due to the paddle fan, the time taken for infectious particles to decay will be compared to the time that air particles are expected to be in the upper room space. Solving (3.14) gives that the time taken for infectious particles to decay is $\tau = \frac{1}{k_i H_i}$, which for this experiment was 203 seconds. While the time that air particles are expected to be in the upper room space is $\left(\frac{V_{Uw}}{V_w} \cdot air turnover rate\right)^{-1}$, which for this experiment was 480 seconds. This means that on each circulation of air in the room, it is expected that $\left(1 - e^{-480/203}\right) = 90.6\%$ of the infectious particles in that air will decay. Considering that approximately ten units of air are circulated per unit of air that is extracted from the room, it is concluded that there is sufficient contact time of the upper room GUV irradiation with the infectious particles.

A potential reason for the difference in expected to experimental results could be as a result of unmodelled dynamics of the disease manifestation. It could be that the actual number of infected in animal room two is under-represented by the last diagnosis. To remove some of the uncertainty regarding the incubation period, and unmodelled dynamics revolving around this, it is recommended that the sentinel animals be kept for another month after the end of the exposure to ward air. This has been done in a previous experiment [70], and is now the standard that is used by the AIR facility.

Although the guinea pig and TST is still the most relevant clinical endpoint [122], a difficulty exists with using guinea pig TST results as the measurement for the number of infected. Because the TST cannot be conducted at higher frequency intervals, only three data points per animal room are available for this experiment. This makes it impossible to ensure that the data is a perfect representation of the actual trend. It is unknown whether data points are slightly skewed through the natural variation that results from slightly different responses to the exposure of the ward air by different animals. Using a large number of guinea pigs for an experiment does reduce the risk of the data not showing the true mean. Therefore, the AIR facility does try to ensure that an adequate number of guinea pigs is used in

the experiments conducted to give a representative sample of the number of infected. The TST is also still the best method of indicating infection in the guinea pigs.

The simulation results depict the expected results of fewer infections in animal room one well, as can be seen from Figure 4.7. This implies it is unlikely the fluctuations in airflow and the disruptions from power outages resulted in the experiment producing the unexpected results of more infections in animal room one. This is because the airflow rate data (Figures 4.3 and 4.4) and GUV switching data (Figure 4.5) were taken from the SCADA system. Therefore, the fluctuations in airflow and the disruptions from power outages were directly incorporated in the simulation outcome.

The simulation also indicates the dynamic effects of the GUV lamp switching on the infectious particles is much faster than the switching cycle of air between animal rooms. This can be seen from Figures 5.2 and 5.3, where there appears to be a spike in the infectious particles entering animal room one whenever ward air is switched to this animal room. These spikes are caused by the time taken by the GUV lamps to reduce the number of infectious particles in the ward, and hence the rate of infectious particles transferred to animal room one. This implies the unexpected experiment results are unlikely to be caused by the change in steady-state of the infectious particles in the ward that happens after switching the state of the GUV lamps.

Based on these observations, it is the opinion of the author, that the unexpected experimental results were not caused due to negligence on the part of the AIR facility. The phenomenon observed is not yet understood, and will require further investigation.

CHAPTER 6 CONCLUSION

Mathematics is a concise language with well-defined rules for manipulation. A mathematical model of a system is a useful tool to help with the understanding of the problem and with the theoretical exploration of ideas. The given framework description on the risk of transmission of an airborne infectious disease in indoor spaces is modular in nature. This makes the modelling process simpler through the presentation of different mechanisms and how these mechanisms can be combined to describe different situations. The given approach was demonstrated through the simulation of an experiment, conducted at the AIR facility from 31 August 2015 to 4 December 2015.

The simulation helped investigate potential reasons for the experiment not producing the results that were expected. Although the cause of the experiment not producing expected results was not ascertained, it was found that it was not due to an oversight on the part of the AIR facility. This indicates that there is some mechanism or dynamic surrounding the risk of transmission of tuberculosis that is not yet fully understood, and requires further research. The sensitivity analysis further shows that accurate simulation predictions are challenging to achieve when using the quanta of infection unit, due to very large uncertainty surrounding the quanta generation rate.

6.1 CONCLUDING REMARKS

Through the time spent studying, investigating, researching and modelling tuberculosis, it is clear that the control engineering contribution that can be made to the study of this infectious disease is very different than that to HIV [19]. This research began thinking to replicate the work done with HIV, but only on a different disease. This implied investigating the immunological response to tuberculosis, obtaining a suitable model, and using the treatment as a control handle. However, this thinking turned out to be erroneous.

Control theory is a useful tool when investigating a topic in the universal language of mathematics. However, to apply effective control, a degree of freedom in manipulated variables is required, and another major requirement is that of information or measurement. On both these fronts there were significant challenges when considering tuberculosis.

On the requirement of information, TB is diagnosed as positive or negative, with no real quantitative data on the level of TB. Sputum analysis does give a bacterial load ranking; however, there are some issues even with this. Firstly, this information can be highly dependent on the manner in which the sputum was obtained; how the patient coughed when generating the sputum, and from which site of infection in the lungs is the sputum. Secondly, the sputum takes a long time to culture (15-20 days). The only other real manner to obtain a quantitative measurement of bacterial loads, would be to perform a bronchoscopy on the patient. This procedure involves putting the patient under general anaesthetic, manoeuvring the bronchoscope down the throat, and taking a swab of the lung. However, the risks of the procedure far outweigh any value in obtaining the quantitative bacterial loads.

On the requirement for manipulated variables, the treatment regime is a poor handle. The World Health Organisation (WHO) dictates conservative standard practices, and the risk of antibiotic resistance forming would outweigh any slight cost benefit in optimising this regime. Treatment is begun as soon as diagnosis is made, and the challenge in public heath is more on the side of diagnosing tuberculosis early, rather than a question of when to initiate therapy.

However, this is only looking at the contribution that control engineering can do on the individual's level of abstraction, in terms of system biology [123]. On the population level, slightly more control handles present themselves. However, there is probably only a very small niche area in which this contribution can be made, as the investigation of the population level falls into the domain of epidemiology. Therefore, to not just replicate an epidemiological study, but to add a contribution, the dynamics of the 'system' would need to be investigated.

This work has set the foundation to attempt a contribution in this niche area, by starting the process of being able to build a population level model, where the dynamics of control actions, such as environmental influences or upper room germicidal ultraviolet irradiation can make an impact. However, this does depend on the measurements available to allow for improved control.

6.2 RESEARCH QUESTION ANSWERS

Although the research question of why the experiment conducted at the AIR facility did not produce the expected result, it can be stated the unexpected experimental results were not caused due to negligence on the part of the AIR facility. The phenomenon observed is not yet understood, and will require further investigation.

This indicates that there is some mechanism or dynamic surrounding the risk of transmission of tuberculosis that is not yet fully understood, and requires further research. The sensitivity analysis further shows that accurate simulation predictions are challenging to achieve when using the quanta of infection unit, due to very large uncertainty surrounding the quanta generation rate.

6.3 SUGGESTIONS FOR FURTHER WORK

- Investigate the experiment from a biological perspective for a deeper rationale of why the experiment did not produce the expected outcome.
- Develop a state estimator that can give an estimation of the number of bacilli present. This could be a useful tool to be used in health care facilities as a method of indicating when a facility is at risk. (What state feedback would be available? Would there be a method to determine the number of infected individuals as an automated measurement? Perhaps the measurement of carbon dioxide as an indication of re-breathed air could prove useful for this.)
- If the bacilli measurement is assumed to be available, could the number of infected individuals be estimated? (For example through a state estimator.) Other measurement data, such as carbon dioxide levels might assist in this.
- Develop a Model Predictive Controller that always minimises the risk of transmission, while at the same time optimises on the environmental comfort (chill factor) that patients may experience.
- Develop a Model Predictive Controller that always minimises the risk of transmission, while at the same time tries to reduce the energy cost of a heating, ventilation and air-conditioning (HVAC) system.
- Is there benefit of 'blasting' a whole room with high intensity UV light when no people are detected to be present?
- Can the transmission mechanisms discussed in this text be extended to a population level with localised clusters? (Perhaps by classifying nodes in the network as different zones that people

move in between.) Then can these population models be used to identify where intervention of environmental controls would be most effective? (Maybe if an area is identified as having high prevalence, what is the impact of focusing on these public locations? What dynamics can be manipulated to help with the public health intervention with this?)

- Model Predictive Control (MPC) of a population, where assumptions can be made that a focus on public intervention leads to quicker diagnosis (reduce the period that infector spreads the disease without knowing about it), quicker treatment (assume that an infector becomes non-contagious after a short period, usually about two weeks to a month after starting treatment). However, public intervention is constrained through cost. The public intervention can come in various forms: education, better access to facilities for diagnosis (mobile TB clinics?), and better access to drugs. Environmental control factors could also be considered, such as distribution of GUV lights. Disturbances can come from reactivation of latent TB.
- If the population model is converted into a probability based model for the 'actual' plant, how does Model Predictive Control (MPC) fair with a probability based model? It might be necessary to still have the model of the MPC controller be continuous, even when the model of the 'actual' plant is probability based.

REFERENCES

[1] K. Lönnroth, K. G. Castro, J. M. Chakaya, L. S. Chauhan, K. Floyd, P. Glaziou, and M. C. Raviglione, "Tuberculosis control and elimination 2010–50: cure, care, and social development," *The Lancet*, vol. 375, no. 9728, pp. 1814–1829, May 2010.

[2] S. S. A. Karim, G. J. Churchyard, Q. A. Karim, and S. D. Lawn, "HIV infection and tuberculosis in South Africa: an urgent need to escalate the public health response," *The Lancet*, vol. 374, no. 9693, pp. 921–933, September 2009.

[3] C. Dye, P. Glaziou, K. Floyd, and M. Raviglione, "Prospects for Tuberculosis Elimination," *Annual Review of Public Health*, vol. 34, no. 1, pp. 271–286, March 2013.

[4] T. A. Yates, P. Y. Khan, G. M. Knight, J. G. Taylor, T. D. McHugh, M. Lipman, R. G. White, T. Cohen, F. G. Cobelens, R. Wood, D. A. J. Moore, and I. Abubakar, "The transmission of Mycobacterium tuberculosis in high burden settings," *The Lancet Infectious Diseases*, vol. 16, no. 2, pp. 227–238, February 2016.

[5] S. K. Schwander and J. Ellner, "The human host: immunology and susceptibility," in *Reichman and Hershfield's Tuberculosis, Part A: A Comprehensive, International Approach*, 3rd ed., M. C. Raviglione and C. S. Lambregts, Eds. London: CRC Press, 2006, ch. 6, pp. 117–154.

[6] World Health Organisation, *International standards for tuberculosis care*, 3rd ed. Hague: TB CARE 1, 2014.

[7] P. Sudre, G. ten Dam, and A. Kochi, "Tuberculosis: a global overview of the situation today." *Bulletin of the World Health Organization*, vol. 70, no. 6, pp. 149–159, 1992.

[8] C. Dye, S. Scheele, P. Dolin, P. Vikram, and M. C. Raviglione, "Global burden of tuberculosis: Estimated incidence, prevalence, and mortality by country," *Journal of American Medical Association*, vol. 282, no. 7, pp. 677–686, August 1999.

[9] J. Goudge, L. Gilson, S. Russell, T. Gumede, and A. Mills, "Affordability, availability and acceptability barriers to health care for the chronically ill: longitudinal case studies from South Africa." *BMC Health Services Research*, vol. 9, no. 75, pp. 1–18, January 2009.

[10] E. Nardell and A. S. Dharmadhikari, "Turning off the spigot: reducing drug-resistant tuberculosis transmission in resource-limited settings," *International Journal of Tuberculosis and Lung Disease*, vol. 14, no. 10, pp. 1233–1243, 2010.

[11] C. M. Yuen, F. Amanullah, A. Dharmadhikari, E. A. Nardell, J. A. Seddon, I. Vasilyeva, Y. Zhao, S. Keshavjee, and M. C. Becerra, "Turning off the tap: stopping tuberculosis transmission through active case-finding and prompt effective treatment," *The Lancet*, vol. 386, no. 10010, pp. 2334–2343, December 2015.

[12] E. A. Nardell, "Indoor environmental control of tuberculosis and other airborne infections," *Indoor Air*, vol. 26, no. 1, pp. 79–87, February 2016.

[13] E. Mupere, N. K. Schiltz, E. Mulogo, A. Katamba, J. Nabbuye-Sekandi, and M. E. Singer, "Effectiveness of active case-finding strategies in tuberculosis control in Kampala, Uganda," *The International Journal of Tuberculosis and Lung Disease*, vol. 17, no. 2, pp. 207–213, February 2013.

[14] C. B. Beggs, J. K. Donnelly, K. G. Kerr, P. A. Sleigh, D. D. Mara, and G. Cairns, "The use of engineering controls to disinfect Mycobacterium tuberculosis and airborne pathogens in hospital buildings," *Indoor and Built Environment*, vol. 9, no. 1, pp. 17–27, 2000.

[15] Y. Li, G. M. Leung, J. W. Tang, X. Yang, C. Y. H. Chao, J. Z. Lin, J. W. Lu, P. V. Nielsen, J. Niu,

H. Qian, A. C. Sleigh, H.-J. J. Su, J. Sundell, T. W. Wong, and P. L. Yuen, "Role of ventilation in airborne transmission of infectious agents in the built environment - a multidisciplinary systematic review," *Indoor Air*, vol. 17, no. 1, pp. 2–18, February 2007.

[16] A. S. Dharmadhikari, M. Mphahlele, K. Venter, A. Stoltz, R. Mathebula, T. Masotla, M. van der Walt, M. Pagano, P. Jensen, and E. Nardell, "Rapid impact of effective treatment on transmission of multidrug-resistant tuberculosis," *International Journal of Tuberculosis and Lung Disease*, vol. 18, no. 9, pp. 1019–1025, 2014.

[17] G. N. Sze To and C. Y. H. Chao, "Review and comparison between the Wells-Riley and dose-response approaches to risk assessment of infectious respiratory diseases," *Indoor Air*, vol. 20, no. 1, pp. 2–16, 2010.

[18] A. Jeffrey, Xiaohua Xia, and I. Craig, "When to initiate HIV therapy: a control theoretic approach," *IEEE Transactions on Biomedical Engineering*, vol. 50, no. 11, pp. 1213–1220, November 2003.

[19] I. K. Craig and X. Xia, "Can HIV/AIDS be controlled? Applying control engineering concepts outside traditional fields," *IEEE Control Systems Magazine*, vol. 25, no. 1, pp. 80–83, February 2005.

[20] P. Antsaklis, "Defining intelligent control," *IEEE Control Systems Magazine*, vol. 4, no. 5, pp. 58–66, June 1994.

[21] B. Müller, S. Dürr, S. Alonso, J. Hattendorf, C. J. M. Laisse, S. D. C. Parsons, P. D. van Helden, and J. Zinsstag, "Zoonotic Mycobacterium bovis - induced tuberculosis in humans." *Emerging Infectious Diseases*, vol. 19, no. 6, pp. 899–908, 2013.

[22] S. Lapage, P. Sneath, E. Lessel, V. Skerman, H. Seeliger, and W. Clark, *International Code of Nomenclature of Bacteria*. ASM Press, 1992.

[23] T. Cavalier-Smith, "A revised six-kingdom of life," *Biological Reviews*, vol. 73, no. 3, pp. 203–266, 1998.

[24] E. R. Angert, “Alternatives to binary fission in bacteria,” *Nature Reviews Microbiology*, vol. 3, no. 3, pp. 214–224, 2005.

[25] E. Stackebrandt, F. Rainey, and N. L. Ward-Rainey, “Proposal for a new hierarchic classification system, Actinobacteria classis nov.” *International Journal of Systematic Bacteriology*, vol. 47, no. 2, pp. 479–491, 2017.

[26] G. J. Hucker and H. J. Conn, “Methods of gram staining,” *Technical Bulletin of the New York State Agricultural Experiment Station*, vol. 23, no. March, pp. 1–37, 1923.

[27] F. G. Winder and P. B. Collins, “Inhibition by Isoniazid of Synthesis of Mycolic Acids in Mycobacterium tuberculosis,” *Journal of General Microbiology*, vol. 63, no. 1, pp. 41–48, 1970.

[28] N. Rastogi, E. Legrand, and C. Sola, “The mycobacteria : an introduction to nomenclature and pathogenesis,” *Revue Scientifique Et Technique*, vol. 20, no. 1, pp. 21–54, 2001.

[29] O. Cosivi, J. M. Grange, C. J. Daborn, M. C. Raviglione, T. Fujikura, D. Cousins, R. A. Robinson, H. F. Huchzermeyer, I. De Kantor, and F. X. Meslin, “Zoonotic tuberculosis due to Mycobacterium bovis in developing countries,” *Emerging Infectious Diseases*, vol. 4, no. 1, pp. 59–70, 1998.

[30] A. Somoskovi, J. Dormandy, A. R. Mayrer, M. Carter, N. Hooper, and M. Salfinger, “"Mycobacterium canettii" isolated from a human immunodeficiency virus-positive patient: First case recognized in the United States,” *Journal of Clinical Microbiology*, vol. 47, no. 1, pp. 255–257, 2009.

[31] S. Rodríguez, J. Bezos, B. Romero, L. de Juan, J. Álvarez, E. Castellanos, N. Moya, F. Lozano, M. Tariq Javed, J. L. Sáez-Llorente, E. Liébana, A. Mateos, L. Domínguez, and A. Aranaz, “Mycobacterium caprae infection in livestock and wildlife, Spain,” *Emerging Infectious Diseases*, vol. 17, no. 3, pp. 532–535, 2011.

[32] K. A. Alexander, P. N. Laver, A. L. Michel, M. Williams, P. D. van Helden, R. M. Warren, and N. C. van Pittius, “Novel mycobacterium tuberculosis complex pathogen, M. Mungi,” *Emerging*

Infectious Diseases, vol. 16, no. 8, pp. 1296–1299, 2010.

[33] J. van Ingen, Z. Rahim, A. Mulder, M. J. Boeree, R. Simeone, R. Brosch, and D. van Soolingen, "Characterization of Mycobacterium orygis as M. tuberculosis complex subspecies," *Emerging Infectious Diseases*, vol. 18, no. 4, pp. 653–655, 2012.

[34] D. V. Cousins, R. Bastida, A. Cataldi, V. Quse, S. Redrobe, S. Dow, P. Duignan, A. Murray, C. Dupont, N. Ahmed, D. M. Collins, W. R. Butler, D. Dawson, D. Rodríguez, J. Loureiro, M. I. Romano, A. Alito, M. Zumarraga, and A. Bernardelli, "Tuberculosis in seals caused by a novel member of the Mycobacterium tuberculosis complex: Mycobacterium pinnipedii sp. nov," *International Journal of Systematic and Evolutionary Microbiology*, vol. 53, no. 5, pp. 1305–1314, 2003.

[35] S. D. C. Parsons, J. A. Drewe, N. C. G. van Pittius, R. M. Warren, and P. D. van Helden, "Novel cause of tuberculosis in meerkats, South Africa," *Emerging Infectious Diseases*, vol. 19, no. 12, pp. 2004–2007, 2013.

[36] Y. C. Manabe, A. M. Dannenberg, S. K. Tyagi, C. L. Hatem, M. Yoder, S. C. Woolwine, B. C. Zook, M. L. M. Pitt, and W. R. Bishai, "Different Strains of Mycobacterium tuberculosis Cause Various Spectrums of Disease in the Rabbit Model of Tuberculosis," *Infection and Immunity*, vol. 71, no. 10, pp. 6004–6011, October 2003.

[37] M. D. Iseman, "Evolution of drug-resistant tuberculosis: a tale of two species," *Proceedings of the National Academy of Sciences of the United States of America*, vol. 91, no. 7, pp. 2428–2429, 1994.

[38] T. Brown, V. Nikolayevskyy, P. Velji, and F. Drobniewski, "Associations between Mycobacterium tuberculosis strains and phenotypes," *Emerging Infectious Diseases*, vol. 16, no. 2, pp. 272–280, 2010.

[39] T. Smith, K. A. Wolff, and L. Nguyen, "Molecular Biology of Drug Resistance in Mycobacterium tuberculosis," in *Life Science Journal*, 2012, vol. 6, no. 4, pp. 53–80.

[40] W. F. Wells, *Airborne Contagion and Air Hygiene*. Cambridge: Cambridge University Press, 1955.

[41] K. P. Fennelly, J. W. Martyny, K. E. Fulton, I. M. Orme, D. M. Cave, and L. B. Heifets, "Cough-generated Aerosols of Mycobacterium tuberculosis," *American Journal of Respiratory and Critical Care Medicine*, vol. 169, no. 5, pp. 604–609, March 2004.

[42] S. Bhangar, J. A. Huffman, and W. W. Nazaroff, "Size-resolved fluorescent biological aerosol particle concentrations and occupant emissions in a university classroom," *Indoor Air*, vol. 24, no. 6, pp. 604–617, December 2014.

[43] S. Yang, G. W. Lee, C.-M. Chen, C.-C. Wu, and K.-P. Yu, "The Size and Concentration of Droplets Generated by Coughing in Human Subjects," *Journal of Aerosol Medicine*, vol. 20, no. 4, pp. 484–494, December 2007.

[44] J. Tang, Y. Li, I. Eames, P. Chan, and G. Ridgway, "Factors involved in the aerosol transmission of infection and control of ventilation in healthcare premises," *Journal of Hospital Infection*, vol. 64, no. 2, pp. 100–114, October 2006.

[45] K. Schwartzman and D. Menzies, "How Long Are TB Patients Infectious?" *Canadian Medical Association Journal*, vol. 163, no. 2, pp. 157–158, 2000.

[46] D. G. Storla, S. Yimer, and G. A. Bjune, "A systematic review of delay in the diagnosis and treatment of tuberculosis," *BMC Public Health*, vol. 8, no. 1, p. 15, 2008.

[47] E. C. Jones-López, O. Namugga, F. Mumbowa, M. Ssebidandi, O. Mbabazi, S. Moine, G. Mboowa, M. P. Fox, N. Reilly, I. Ayakaka, S. Kim, A. Okwera, M. Joloba, and K. P. Fennelly, "Cough aerosols of Mycobacterium tuberculosis predict new infection: A household contact study," *American Journal of Respiratory and Critical Care Medicine*, vol. 187, no. 9, pp. 1007–1015, 2013.

[48] I. Smith, "Mycobacterium tuberculosis pathogenesis and molecular determinants of virulence," *Clinical Microbiology Reviews*, vol. 16, no. 3, pp. 463–496, 2003.

[49] J. A. Philips and J. D. Ernst, "Tuberculosis Pathogenesis and Immunity," *Annual Review of Pathology: Mechanisms of Disease*, vol. 7, no. 1, pp. 353–384, 2012.

[50] A. Perelson and G. Weisbuch, "Immunology for physicists," *Reviews of Modern Physics*, vol. 69, no. 4, pp. 1219–1267, October 1997.

[51] S. H. Kaufmann, "How can immunology contribute to the control of tuberculosis?" *Nature reviews. Immunology*, vol. 1, no. 1, pp. 20–30, October 2001.

[52] A. Raja, "Immunology of tuberculosis," *Indian Journal of Medical Research*, vol. 120, no. 4, pp. 213–232, October 2004.

[53] G. Magombedze, W. Garira, and E. Mwenje, "Modelling the human immune response mechanisms to Mycobacterium tuberculosis infection in the lungs," *Mathematical Biosciences and Engineering*, vol. 3, no. 4, pp. 661–682, October 2006.

[54] P. Chandrasoma and C. R. Taylor, *Concise pathology*, 3rd ed. New York: McGraw-Hill, 1998.

[55] J. M. Tufariello, J. Chan, and J. L. Flynn, "Latent tuberculosis: mechanisms of host and bacillus that contribute to persistent infection," *The Lancet. Infectious diseases*, vol. 3, no. 9, pp. 578–90, September 2003.

[56] E. Corbett, C. Watt, N. Walker, D. Maher, B. Williams, M. Raviglione, and C. Dye, "The growing burden of tuberculosis: Global trends and interactions with the HIV epidemic," *Archives of Internal Medicine*, vol. 163, no. 9, pp. 1009–1021, May 2003.

[57] D. C. M. Angela Houston, "Extrapulmonary tuberculosis," *Medicine*, vol. 42, no. 1, pp. 18–22, 2014.

[58] M. P. Golden and H. R. Vikram, "Extrapulmonary tuberculosis: An overview," *American Family Physician*, vol. 72, no. 9, pp. 1761–1768, 2005.

[59] K. Siddiqi, M. L. Lambert, and J. Walley, "Clinical diagnosis of smear-negative pulmonary tuberculosis in low-income countries: The current evidence," *Lancet Infectious Diseases*, vol. 3, no. 5, pp. 288–296, 2003.

[60] World Health Organization, "Treatment of tuberculosis guidelines," Tech. Rep., 2009.

[61] M. Porta, S. Greenland, M. Hernán, I. dos Santos Silva, and J. M. Last, *A dictionary of epidemiology*, 6th ed., M. Porta, Ed. Oxford University Press, 2014.

[62] World Health Organization, "Global tuberculosis report 2018," Tech. Rep., 2018.

[63] R. M. Houben and P. J. Dodd, "The Global Burden of Latent Tuberculosis Infection: A Re-estimation Using Mathematical Modelling," *PLoS Medicine*, vol. 13, no. 10, pp. 1–13, 2016.

[64] R. M. Merrill, *Introduction to epidemiology*, 7th ed. Jones & Bartlett Learning, 2016.

[65] A. S. Dharmadhikari and E. A. Nardell, "What animal models teach humans about tuberculosis," *American Journal of Respiratory Cell and Molecular Biology*, vol. 39, no. 5, pp. 503–508, 2008.

[66] R. L. Riley, C. C. Mills, F. O'Grady, L. U. Sultan, F. Wittstadt, and D. N. Shivpuri, "Infectiousness of Air from a Tuberculosis Ward," *American Review of Respiratory Disease*, vol. 85, no. 4, pp. 511–525, April 1962.

[67] R. Riley, C. Mills, W. Nyka, N. Weinstock, P. Storey, L. Sultan, M. Riley, and W. Wells, "Aerial dissemination of pulmonary tuberculosis: a two-year study of contagion in a tuberculosis ward," *American Journal of Hygiene*, vol. 70, no. 2, pp. 185–196, February 1959.

[68] E. A. Nardell, "Catching Droplet Nuclei," *American Journal of Respiratory and Critical Care Medicine*, vol. 169, no. 5, pp. 553–554, March 2004.

[69] A. R. Escombe, C. Oeser, R. H. Gilman, M. Navincopa, E. Ticona, C. Martinez, L. Caviedes, P. Sheen, A. Gonzalez, C. Noakes, D. A. J. Moore, J. S. Friedland, and C. A. Evans, "The Detection of Airborne Transmission of Tuberculosis from HIV-Infected Patients, Using an In

Vivo Air Sampling Model," *Clinical Infectious Diseases*, vol. 44, no. 10, pp. 1349–1357, May 2007.

[70] A. S. Dharmadhikari, R. J. Basaraba, M. L. van der Walt, K. Weyerd, M. Mphahlele, K. Venter, P. A. Jensen, M. W. First, S. Parsons, D. N. McMurray, I. M. Orme, and E. A. Nardell, "Natural Infection of guinea pigs exposed to patients with highly drug-resistant tuberculosis," *Tuberculosis*, vol. 91, no. 4, pp. 329–338, 2011.

[71] E. A. Nardell, "Wells Revisited: Infectious Particles vs. Quanta of Mycobacterium tuberculosis Infection – Don't Get Them Confused," *Mycobacterial Diseases*, vol. 6, no. 5, pp. 5–7, 2016.

[72] R. L. Riley, "Airborne infection," *American Journal of Medicine*, vol. 57, no. 3, pp. 466–475, 1974.

[73] C. J. Noakes and P. A. Sleigh, "Applying the Wells-Riley equation to the risk of airborne infection in hospital environments: The importance of stochastic and proximity effects," in *Indoor Air 2008: The 11th International Conference on Indoor Air Quality and Climate*, Copenhagen, 2008, pp. 17–22.

[74] R. L. Riley, "What Nobody Needs to Know About Airborne Infection," *American Journal of Respiratory and Critical Care Medicine*, vol. 163, no. 1, pp. 7–8, January 2001.

[75] S. L. Baldwin, C. D'Souza, A. D. Roberts, B. P. Kelly, A. A. Frank, M. A. Lui, J. B. Ulmer, K. Huygen, D. M. McMurray, and I. M. Orme, "Evaluation of new vaccines in the mouse and guinea pig model of tuberculosis," *Infection and Immunity*, vol. 66, no. 6, pp. 2951–2959, 1998.

[76] S. Marino and D. E. Kirschner, "The human immune response to Mycobacterium tuberculosis in lung and lymph node," *Journal of Theoretical Biology*, vol. 227, no. 4, pp. 463–86, April 2004.

[77] D. J. Ordway, C. A. Shanley, M. L. Caraway, E. A. Orme, D. S. Bucy, L. Hascall-Dove, M. Henao-Tamayo, M. R. Harton, S. Shang, D. Ackart, S. L. Kraft, A. J. Lenaerts, R. J.

Basaraba, and I. M. Orme, "Evaluation of standard chemotherapy in the guinea pig model of tuberculosis," *Antimicrobial Agents and Chemotherapy*, vol. 54, no. 5, pp. 1820–1833, 2010.

[78] M. J. Keeling and K. T. D. Eames, "Networks and epidemic models," *Journal of the Royal Society Interface*, vol. 2, no. 4, pp. 295–307, September 2005.

[79] E. F. du Toit and I. K. Craig, "Selective pinning control of the average disease transmissibility in an HIV contact network," *Physical Review E*, vol. 92, no. 1, p. 012810, July 2015.

[80] D. Seborg, T. Edgar, D. Mellichamp, and F. Doyle, *Process dynamics and control*, 3rd ed. New York: John Wiley & Sons, 2011.

[81] N. K. Gupta and R. E. Rink, "Optimum control of epidemics," *Mathematical Biosciences*, vol. 18, no. 3, pp. 383–396, 1973.

[82] A. Heller, "Integrated medical feedback systems for drug delivery," *American Institute of Chemical Engineers Journal*, vol. 51, no. 4, pp. 1054–1066, 2005.

[83] M. Nicas and E. Seto, "A Simulation Model for Occupational Tuberculosis Transmission," *Risk Analysis*, vol. 17, no. 5, pp. 609–616, October 1997.

[84] M. Nicas, "Markov Modeling of Contaminant Concentrations in Indoor Air," *AIHAJ - American Industrial Hygiene Association*, vol. 61, no. 4, pp. 484–491, July 2000.

[85] E. C. Riley, G. Murphy, and R. L. Riley, "Airborne spread of measles in a suburban elementary school," *American Journal of Epidemiology*, vol. 107, no. 5, pp. 421–432, 1978.

[86] F. Doyle, L. Jovanovic, D. Seborg, R. S. Parker, B. W. Bequette, A. M. Jeffrey, X. Xia, I. K. Craig, and T. McAvoy, "A tutorial on biomedical process control," *Journal of Process Control*, vol. 17, pp. 571–572, 2007.

[87] X. Xia, "Estimation of HIV/AIDS parameters," *Automatica*, vol. 39, no. 11, pp. 1983–1988, November 2003.

[88] X. Xia and C. Moog, "Identifiability of nonlinear systems with application to HIV/AIDS models," *IEEE Transactions on Automatic Control*, vol. 48, no. 2, pp. 330–336, February 2003.

[89] R. Filter, X. Xia, and C. Gray, "Dynamic HIV/AIDS Parameter Estimation With Application to a Vaccine Readiness Study in Southern Africa," *IEEE Transactions on Biomedical Engineering*, vol. 52, no. 5, pp. 784–791, May 2005.

[90] L. Gammaitoni, "Using a Mathematical Model to Evaluate the Efficacy of TB Control Measures," *Emerging Infectious Diseases*, vol. 3, no. 3, pp. 335–342, September 1997.

[91] C. B. Beggs, C. J. Noakes, P. A. Sleigh, L. A. Fletcher, and K. Siddiqi, "The transmission of tuberculosis in confined spaces: An analytical review of alternative epidemiological models," *The International Journal of Tuberculosis and Lung Disease*, vol. 7, no. 11, pp. 1015–1026, 2003.

[92] N. S. Nise, "Modelling in the time domain," in *Control Systems Engineering*, 6th ed. Hoboken, New Jersey: John Wiley & Sons, 2011, ch. 3, pp. 118–159.

[93] C. J. Noakes, C. B. Beggs, P. A. Sleigh, and K. G. Kerr, "Modelling the transmission of airborne infections in enclosed spaces," *Epidemiology and Infection*, vol. 134, no. 05, p. 1082, October 2006.

[94] M. Nicas, "Estimating Exposure Intensity in an Imperfectly Mixed Room," *American Industrial Hygiene Association Journal*, vol. 57, no. 6, pp. 542–550, June 1996.

[95] M. Nicas, W. W. Nazaroff, and A. Hubbard, "Toward Understanding the Risk of Secondary Airborne Infection: Emission of Respirable Pathogens," *Journal of Occupational and Environmental Hygiene*, vol. 2, no. 3, pp. 143–154, March 2005.

[96] W. W. Nazaroff, M. Nicas, and S. L. Miller, "Framework for Evaluating Measures to Control Nosocomial Tuberculosis Transmission," *Indoor Air*, vol. 8, no. 4, pp. 205–218, December 1998.

[97] N. J. Ehrenkranz and J. L. Kicklighter, "Tuberculosis outbreak in a general hospital: evidence for airborne spread of infection." *Annals of Internal Medicine*, vol. 77, pp. 377–382, 1972.

[98] J. Fiegel, R. Clarke, and D. A. Edwards, "Airborne infectious disease and the suppression of pulmonary bioaerosols," *Drug Discovery Today*, vol. 11, no. 1-2, pp. 51–57, January 2006.

[99] E. A. Nardell, J. Keegan, S. A. Cheney, and S. C. Etkind, "Airborne infection: Theoretical limits of protection achievable by building ventilation," *American Review of Respiratory Disease*, vol. 144, no. 2, pp. 302–306, 1991.

[100] W. J. Fisk, O. Seppanen, D. Faulkner, and J. Huang, "Economic benefits of an economizer system: Energy savings and reduced sick leave," Tech. Rep., 2004.

[101] M. Nicas, "An Analytical Framework for Relating Dose, Risk, and Incidence: An Application to Occupational Tuberculosis Infection," *Risk Analysis*, vol. 16, no. 4, pp. 527–538, August 1996.

[102] S. Chapman and T. G. Cowling, *The mathematical theory of non-uniform gases: an account of the kinetic theory of viscosity, thermal conduction and diffusion in gases*. Cambridge University Press, 1970.

[103] M.-F. King, C. Noakes, P. Sleigh, and M. Camargo-Valero, "Bioaerosol deposition in single and two-bed hospital rooms: A numerical and experimental study," *Building and Environment*, vol. 59, pp. 436–447, January 2013.

[104] X. Li, K. Inthavong, Q. Ge, and J. Tu, "Numerical investigation of particle transport and inhalation using standing thermal manikins," *Building and Environment*, vol. 60, pp. 116–125, February 2013.

[105] E. S. Mousavi and K. R. Grosskopf, "Ventilation Rates and Airflow Pathways in Patient Rooms: A Case Study of Bioaerosol Containment and Removal," *Annals of Occupational Hygiene*, vol. 59, no. 9, pp. 1190–1199, November 2015.

[106] W. J. Kowalski, W. P. Bahnfleth, D. L. Witham, B. F. Severin, and T. S. Whittam, "Mathematical modeling of ultraviolet germicidal irradiation for air disinfection," *Quantitative Microbiology*, vol. 2, no. 3, pp. 249–270, 2000.

[107] S. L. Miller and J. M. MacHer, "Evaluation of a Methodology for Quantifying the Effect of Room Air Ultraviolet Germicidal Irradiation on Airborne Bacteria," *Aerosol Science and Technology*, vol. 33, no. 3, pp. 274–295, September 2000.

[108] H. L. David, "Response of Mycobacteria to ultraviolet light radiation," *The American Review of Respiratory Disease*, vol. 108, no. 5, pp. 1175–1185, May 1973.

[109] R. L. Riley, M. Knight, and G. Middlebrook, "Ultraviolet susceptibility of BCG and virulent tubercle bacilli," *American Review of Respiratory Disease*, vol. 113, no. 4, pp. 413–418, May 1976.

[110] A. S. Dharmadhikari, M. Mphahlele, A. Stoltz, K. Venter, R. Mathebula, T. Masotla, W. Lubbe, M. Pagano, M. First, P. A. Jensen, M. van der Walt, and E. A. Nardell, "Surgical face masks worn by patients with multidrug-resistant tuberculosis: Impact on infectivity of air on a hospital ward," *American Journal of Respiratory and Critical Care Medicine*, vol. 185, no. 10, pp. 1104–1109, 2012.

[111] M. Mphaphlele, A. S. Dharmadhikari, P. A. Jensen, S. N. Rudnick, T. H. van Reenen, M. A. Pagano, W. Leuschner, T. A. Sears, S. P. Milonova, M. van der Walt, A. C. Stoltz, K. Weyer, and E. A. Nardell, "Institutional tuberculosis transmission: Controlled trial of upper room ultraviolet air disinfection: A basis for new dosing guidelines," *American Journal of Respiratory and Critical Care Medicine*, vol. 192, no. 4, pp. 477–484, 2015.

[112] World Health Organization, *Laboratory biosafety manual*, 3rd ed., Geneva, 2004.

[113] L. F. Shampine, *Numerical solution of ordinary differential equations*. CRC Press, 1994, vol. 4.

[114] L. F. Shampine and M. W. Reichelt, "The MATLAB ODE Suite," *SIAM Journal on Scientific Computing*, vol. 18, no. 1, pp. 1–22, January 1997.

[115] D. Ordway, G. Palanisamy, M. Henao-Tamayo, E. E. Smith, C. Shanley, I. M. Orme, and R. J. Basaraba, "The Cellular Immune Response to Mycobacterium tuberculosis Infection in the Guinea Pig," *The Journal of Immunology*, vol. 179, no. 4, pp. 2532–2541, August 2007.

[116] J. C. Lagarias, J. A. Reeds, M. H. Wright, and P. E. Wright, "Convergence Properties of the Nelder–Mead Simplex Method in Low Dimensions," *SIAM Journal on Optimization*, vol. 9, no. 1, pp. 112–147, January 1998.

[117] J. L. Flynn, "Lessons from experimental Mycobacterium tuberculosis infections," *Microbes and Infection*, vol. 8, no. 4, pp. 1179–1188, April 2006.

[118] K. Sakamoto, "The Pathology of Mycobacterium tuberculosis Infection," *Veterinary Pathology*, vol. 49, no. 3, pp. 423–439, May 2012.

[119] B. G. Liptak, *Instrument Engineers' Handbook, Volume One: Process Measurement and Analysis*. CRC press, 2003.

[120] D. Strydom, R. R. Küsel, and I. K. Craig, "When is it appropriate to model transmission of tuberculosis using a dose response model?" *IFAC-PapersOnLine*, vol. 50, no. 2, pp. 31–36, December 2017.

[121] R. A. Stein, "Super-spreaders in infectious diseases," *International Journal of Infectious Diseases*, vol. 15, no. 8, pp. e510–e513, 2011.

[122] E. A. Nardell, "Air Sampling for Tuberculosis— Homage to the Lowly Guinea Pig," *Chest*, vol. 116, no. 4, pp. 1143–1144, October 1999.

[123] D. Young, J. Stark, and D. E. Kirschner, "Systems biology of persistent infection: Tuberculosis as a case study," *Nature reviews: Microbiology*, vol. 6, no. 7, pp. 520–528, July 2008.

ADDENDUM A AIR MODEL DIFFERENTIAL EQUATION SOLUTION

The solution of the differential equation model of the eMalahleni AIR facility model (4.1) - (4.9) is derived for the case of all parameters being constant over the time period being considered and for an initial zero condition of the infectious particles in the air. The time period considered is assumed to be taken as $[0;t]$.

A.1 INFECTIOUS PARTICLES IN THE WARD

To solve the set of differential equations, the differential equation for the contaminated air in the ward (4.7) will be started with:

$$\frac{dC_w(t)}{dt} = \phi_w I_w - \left(\frac{Q_w}{V_w} + \frac{V_{wU}}{V_w} k_w H_w\right) C_w(t) \quad ,$$

which is rearranged to have the state variable on the left hand side, giving

$$\frac{dC_w(t)}{dt} + \left(\frac{Q_w(t)}{V_w} + \frac{V_{wU}}{V_w} k_w H_w(t)\right) C_w(t) = \phi_w I_w(t) \quad . \tag{A.1}$$

This is a first order linear differential equation and can be solved by integrating both sides of the equation after multiplying with an integration factor. Assuming that the parameters remain constant over the period of time under consideration, the integration factor is obtained to be

$$\exp\left(\int \left(\frac{Q_w}{V_w} + \frac{V_{wU}}{V_w} k_w H_w\right) dt\right) = \exp\left(\left(\frac{Q_w}{V_w} + \frac{V_{wU}}{V_w} k_w H_w\right) t\right) \tag{A.2}$$

Both sides of the equation of (A.1) can be multiplied with the integrating factor (A.2) and then integrated with respect to time.

$$\exp\left(\left(\frac{Q_w}{V_w}+\frac{V_{wU}}{V_w}k_wH_w\right)t\right)C_w(t)=\int\phi_wI_w\exp\left(\left(\frac{Q_w}{V_w}+\frac{V_{wU}}{V_w}k_wH_w\right)t\right)dt+Const$$

$$\exp\left(\left(\frac{Q_w}{V_w}+\frac{V_{wU}}{V_w}k_wH_w\right)t\right)C_w(t)=\frac{\phi I_w\exp\left(\left(\frac{Q_w}{V_w}+\frac{V_{wU}}{V_w}k_wH_w\right)t\right)}{\left(\frac{Q_w}{V_w}+\frac{V_{wU}}{V_w}k_wH_w\right)}+Const$$

$$\therefore C_w(t)=\frac{\phi_wI_w}{\left(\frac{Q_w}{V_w}+\frac{V_{wU}}{V_w}k_wH_w\right)}+Const\times\exp\left(-\left(\frac{Q_w}{V_w}+\frac{V_{wU}}{V_w}k_wH_w\right)t\right)$$

Using the initial condition of $C_w(0)=0$,

$$Const=-\frac{\phi_wI_w}{\left(\frac{Q_w}{V_w}+\frac{V_{wU}}{V_w}k_wH_w\right)}\quad .$$

This then gives

$$C_w(t)=\frac{\phi_wI_w}{\left(\frac{Q_w}{V_w}+\frac{V_{wU}}{V_w}k_wH_w\right)}\left(1-\exp\left(-\left(\frac{Q_w}{V_w}+\frac{V_{wU}}{V_w}k_wH_w\right)t\right)\right)\tag{A.3}$$

A.2 INFECTIOUS PARTICLES IN THE ANIMAL ROOMS

After substituting (A.3) into (4.8) and (4.9), a similar process is followed to derive the time solution to the infectious particles in the animal rooms for an initial zero condition and constant parameters.

$$\frac{dC_i(t)}{dt}=\frac{Q_{iin}}{V_w}C_w(t)-\frac{Q_{iout}}{V_i}C_i(t)\quad ,$$

into which (A.3) is substituted, and the equation rearranged, to give

$$\frac{dC_i(t)}{dt}+\frac{Q_{iout}}{V_i}C_i(t)=\frac{Q_{iin}}{V_w}\left(\frac{\phi_wI_w}{\left(\frac{Q_w}{V_w}+\frac{V_{wU}}{V_w}k_wH_w\right)}\left(1-\exp\left(-\left(\frac{Q_w}{V_w}+\frac{V_{wU}}{V_w}k_wH_w\right)t\right)\right)\right)$$

Simplifying this equation, and letting

$$\Psi_w(t)=1-\exp\left(-\left(\frac{Q_w}{V_w}+\frac{V_{wU}}{V_w}k_wH_w\right)t\right)\quad ,$$

gives

$$\frac{dC_i(t)}{dt}+\frac{Q_{iout}}{V_i}C_i(t)=\frac{\phi_wI_wQ_{iin}\Psi_w(t)}{Q_w+V_{wU}k_wH_w}\tag{A.4}$$

The integrating factor in this case is: $\exp\left(\frac{Q_{iout}}{V_i}t\right)$. The solution to (A.4) is thus:

$$C_i(t) = \frac{\phi_w I_w Q_{iin} V_i}{(V_i Q_w + V_i V_{wU} k_w H_w - V_w Q_{iout}) Q_{iout}} + Const_2 \exp\left(-\left(\frac{Q_{iout}}{V_i}\right)t\right)$$

Using the initial condition of $C_i(0) = 0$,

$$Const_2 = -\frac{\phi_w I_w Q_{iin} V_i}{(V_i Q_w + V_i V_{wU} k_w H_w - V_w Q_{iout}) Q_{iout}} \quad .$$

This then gives

$$C_i(t) = \frac{\phi_w I_w Q_{iin} V_i}{(V_i Q_w + V_i V_{wU} k_w H_w - V_w Q_{iout}) Q_{iout}} \left(1 - \exp\left(-\left(\frac{Q_{iout}}{V_i}\right)t\right)\right) \tag{A.5}$$